Electrochemical Applications of Glass: New Functionalities for a Greener Future

Steve W. Martin

Anson Marston Distinguished Professor in Engineering

Department of Materials Science & Engineering

Iowa State University of Science and Technology

swmartin@iastate.edu

The Carbon Energy Problem…

- Consider the world's energy use…

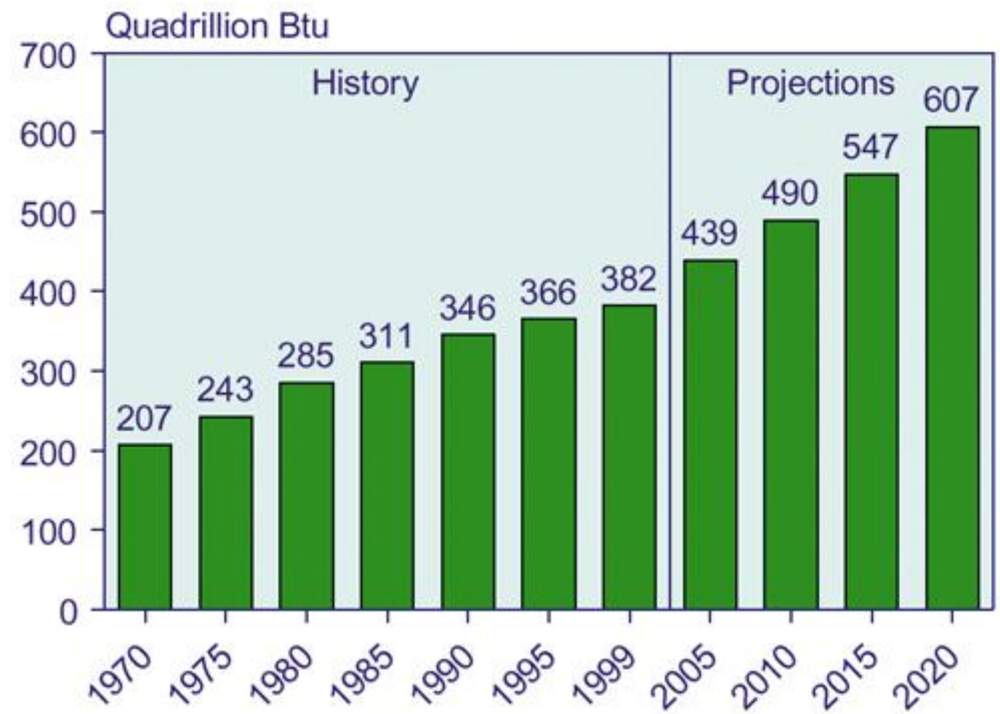

Sources: **History:** Energy Information Administration (EIA), Office of Energy Markets and End Use, International Statistics Database and *International Energy Annual 1999*, DOE/EIA-0219(99) (Washington, DC, January 2001). **Projections:** EIA, World Energy Projection System (2001).

Leading to Increasing World CO_2 Emissions…

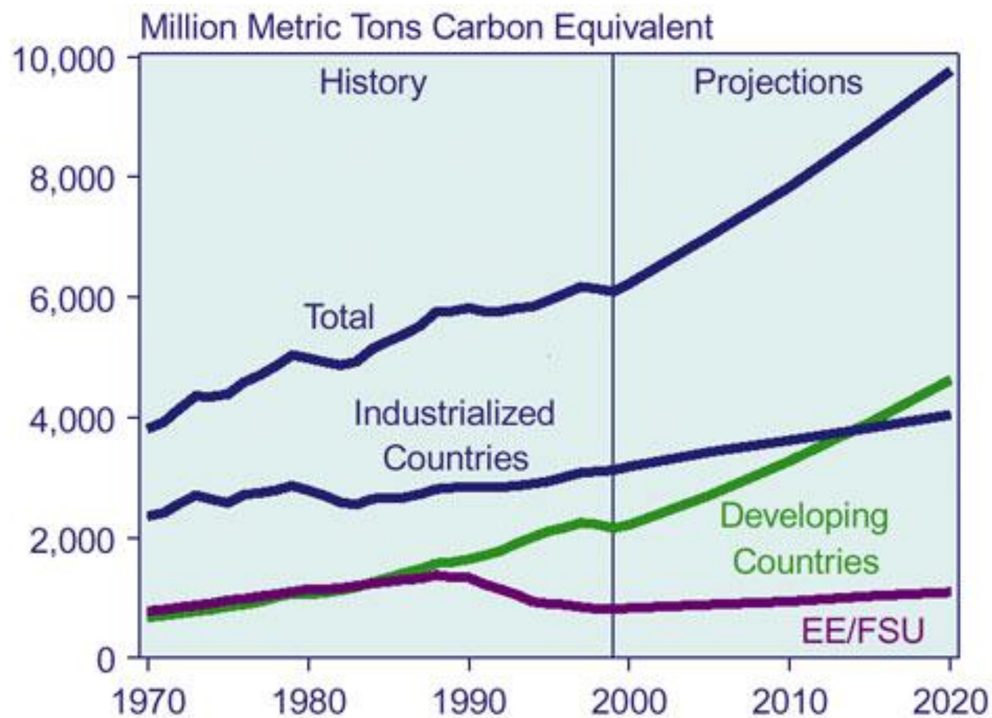

Sources: **History:** Energy Information Administration (EIA), Office of Energy Markets and End Use, International Statistics Database and *International Energy Annual 1999*, DOE/EIA-0219(99) (Washington, DC, January 2001). **Projections:** EIA, World Energy Projection System (2001).

That lead to Global Warming…

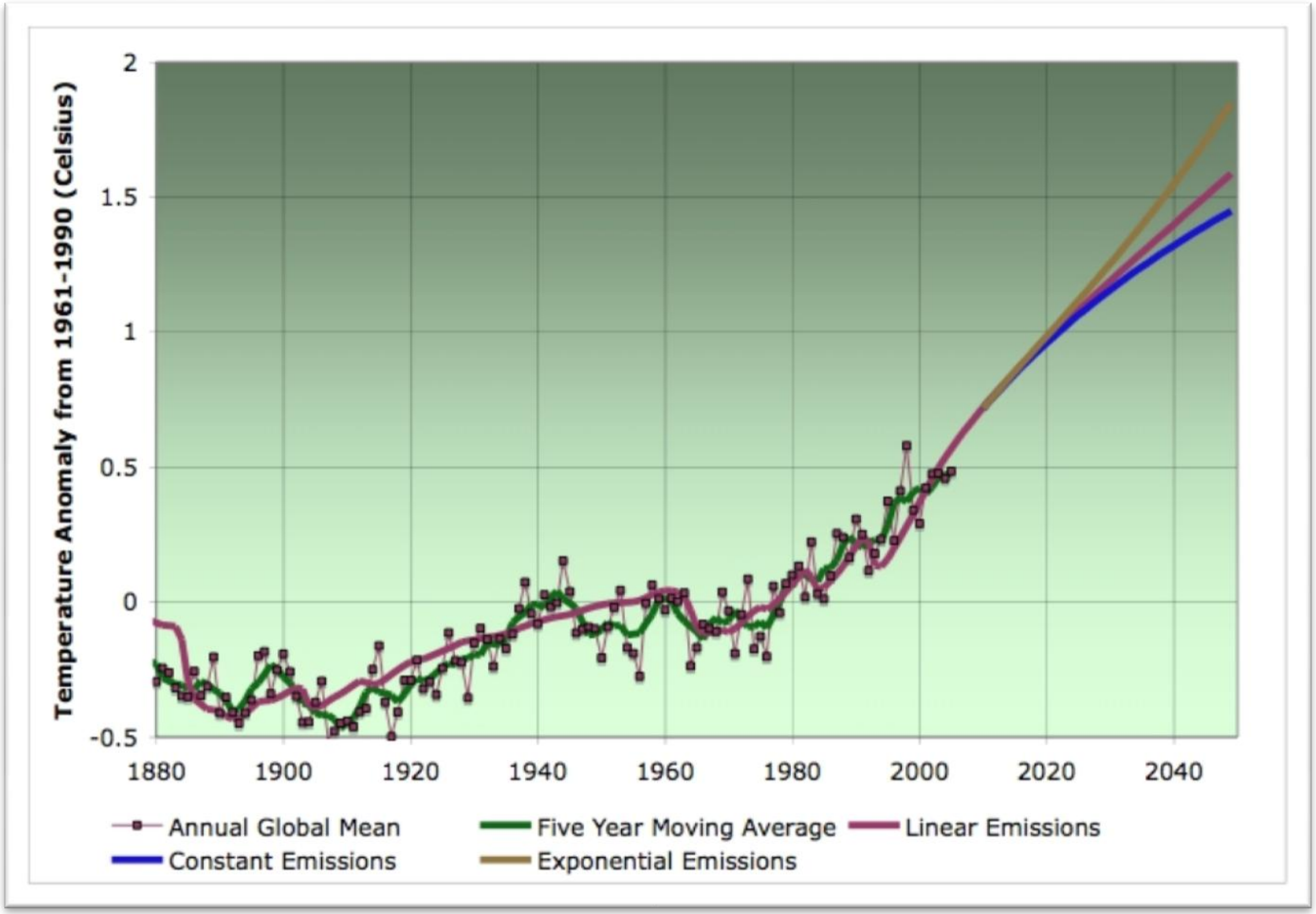

That Suggests Alternative Zero-Carbon Energy Harvesting Systems…such as solar…

Photovoltaic…

Thermal…

Solar source ~ 6,600 TW/year

World use ~ 16 TW/year

…and wind…

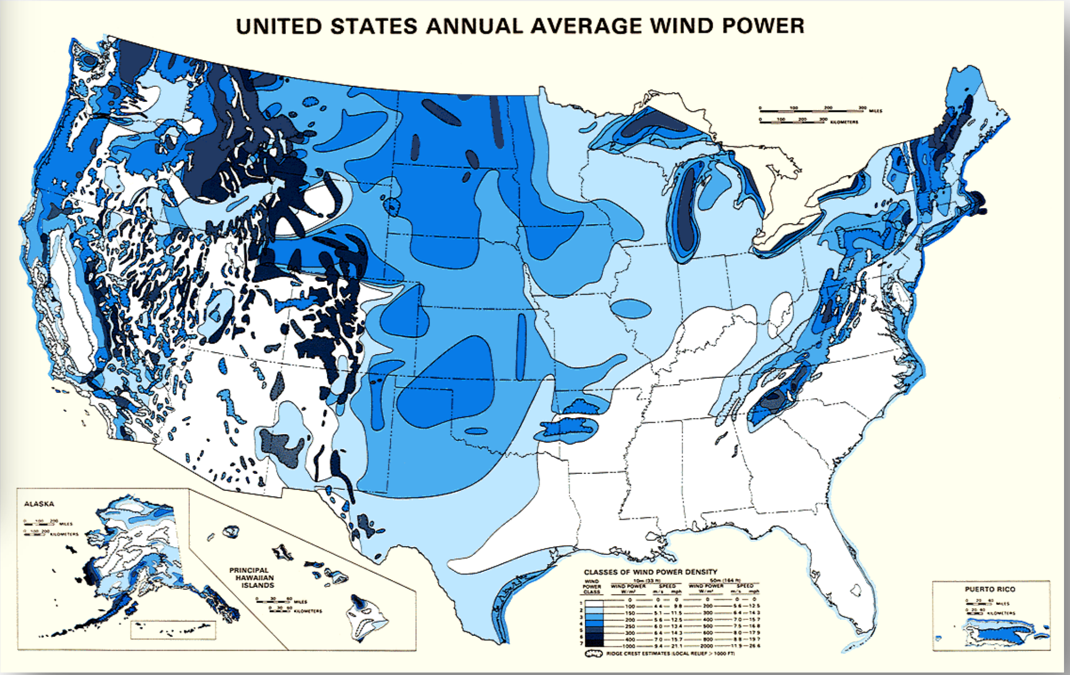
UNITED STATES ANNUAL AVERAGE WIND POWER
ALASKA
PRINCIPAL HAWAIIAN ISLANDS
PUERTO RICO
CLASSES OF WIND POWER DENSITY

However….

- Solar-based energy systems are temporal
- and…Energy demand is temporal
- Energy storage systems are necessary to balance the mismatch between supply and demand
  - Mechanical – pressure, m·g, hydro…
  - Electrical – capacitors…
  - Chemical – batteries…

Further…

- Portable energy is also required for….
  - Transportation
  - Mechanical work
  - Electronics
  - Health care
  - Food production
  - …

Portable energy for transportation…

- Must be developed
- Will be more expensive than oil
- Must be used as efficiently as possible
- Consider the demand…
  - ~8,000 cars and ~150 miles of paved roads in 1900
  - ~600,000,000 passenger cars in 2008
  - ~1,200,000,000 passenger cars expected in 2030
- Will half of all cars be hybrids in 2030?
  - 600,000,000+ battery systems?

Portable energy for personal electronics…

- ~6 Billion people, ~4 billion cell phones in 2008
- In 30 countries, cell phone use now exceeds 100%
  - Italy ~ 122%
  - Sweden ~ 110%
- Consider the demand…
  - ~9 Billion people in 2050?
  - ~10 Billion cell phones?
  - ~10+ Billion Lithium batteries?

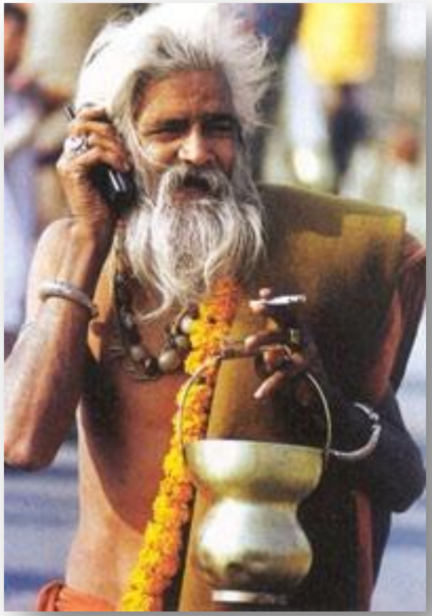

The paradigm has changed….

Thus…Portable Energy Sources are Critical Technologies

But….what's the problem…?

Anode and Cathode Combinations Determine the Voltage and Energy Density of Lithium Batteries

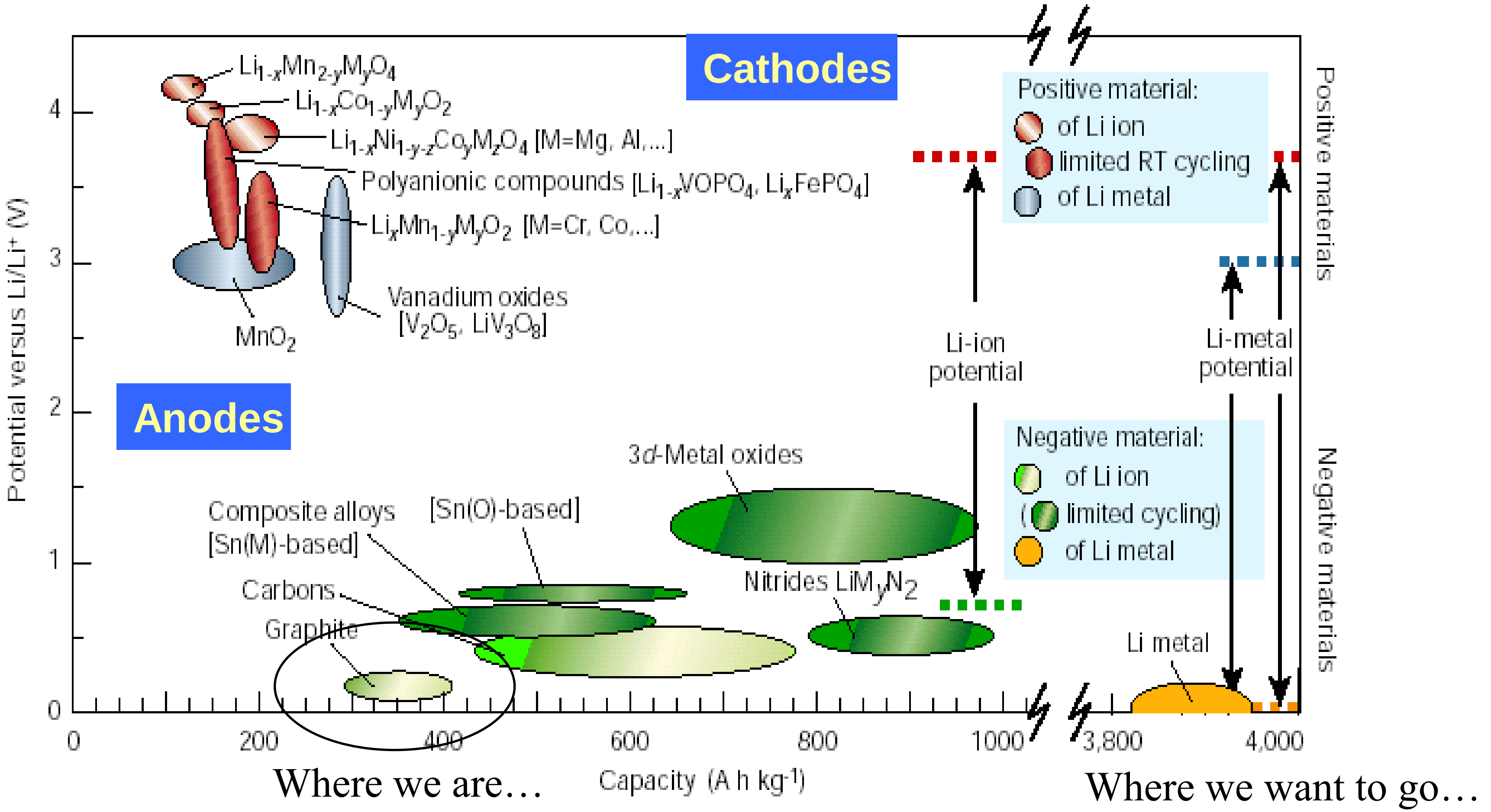

J.M. Tarascon, M. Armand, Nature, 414, 15 (2001) 359

Just for comparison…

Where we are… Where we can go…

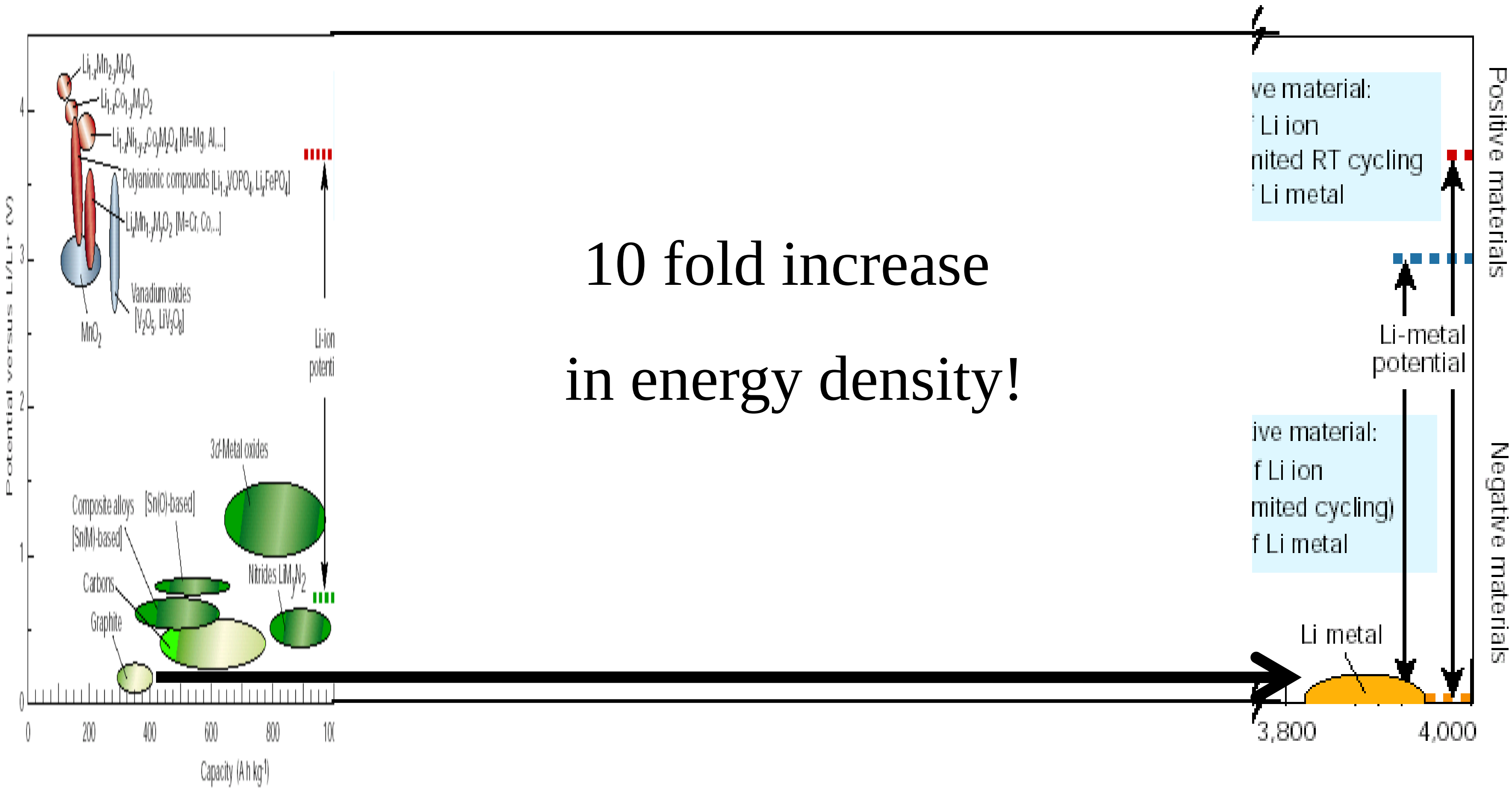

Li-ion Batteries

C_6 is a common anode material for Li-ion batteries

The maximum capacity of graphite (LiC_6): 410Ah/kg
1339 C/g

Good cycle-life

But, Low capacity for new portable devices

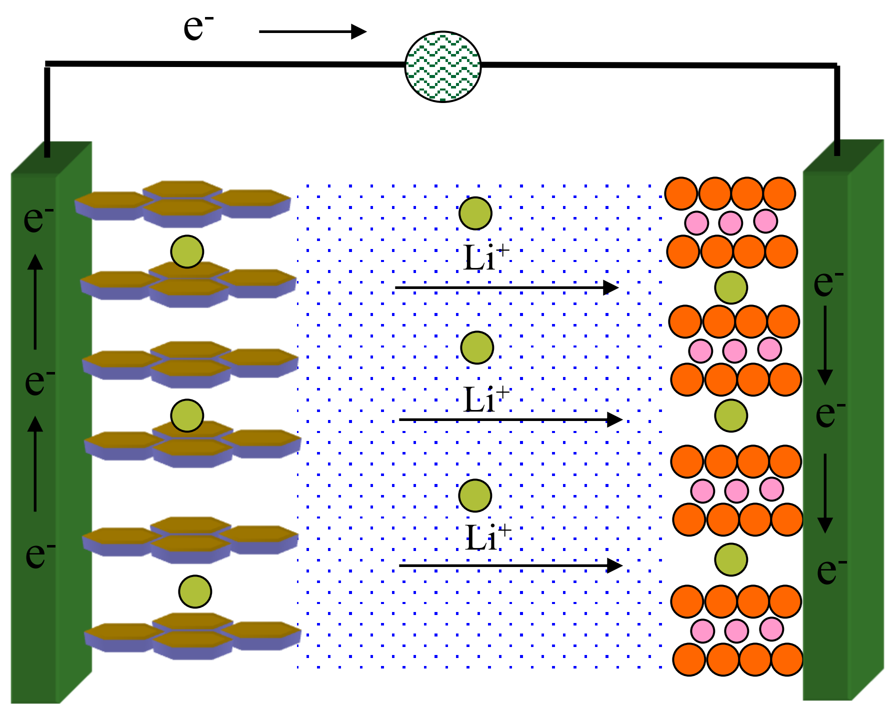

Li_xC_6 Li^+ conducting electrolyte $Li_{1-x}CoO_2$

Anode: $Li_xC_6 \longrightarrow xLi^+ + xe^- + C_6$

Cathode: $Li_{1-x}CoO_2 + xLi^+ + xe^- \longrightarrow LiCoO_2$

New Lithium Battery Designs - Anode

- Higher energy storage in the anode
  - Move closer to unit activity of metallic lithium
  - Yet maintain safety
    - Stability in contact with electrolyte and other battery materials
  - Preference is to manufacture Lithium batteries in the discharged state
    - Does not require handling high activity material
    - Increases shelf life of battery before selling
    - Reduces time and cost of manufacture
    - Increases safety during storage and shipment
    - Increases the lifetime of the battery for the consumer

New Lithium Battery Designs - Anode

- Need a cheap material that will store lithium safely near unit activity that will charge and discharge Li reversibly, ~4000x (~10 years), near 0 V (vs. Li/Li^{+}) at a density near that of Li
- To obtain 50% loss after ~ 10 years, ~4000 cycles, reversibility at each cycle must be ? % reversible?

$$\left(0.9998\right)^{4000} = 0.5$$

Carbon as a Negative Insertion Electrode

- $Li_x C_n \leftrightarrow xLi^+ \; xe^- + C_n$
- x ~ 1, n ~ 6
- C has high e-conductivity
- Cheap
- Plentiful
- Good voltage
- However, relatively low capacity, small x

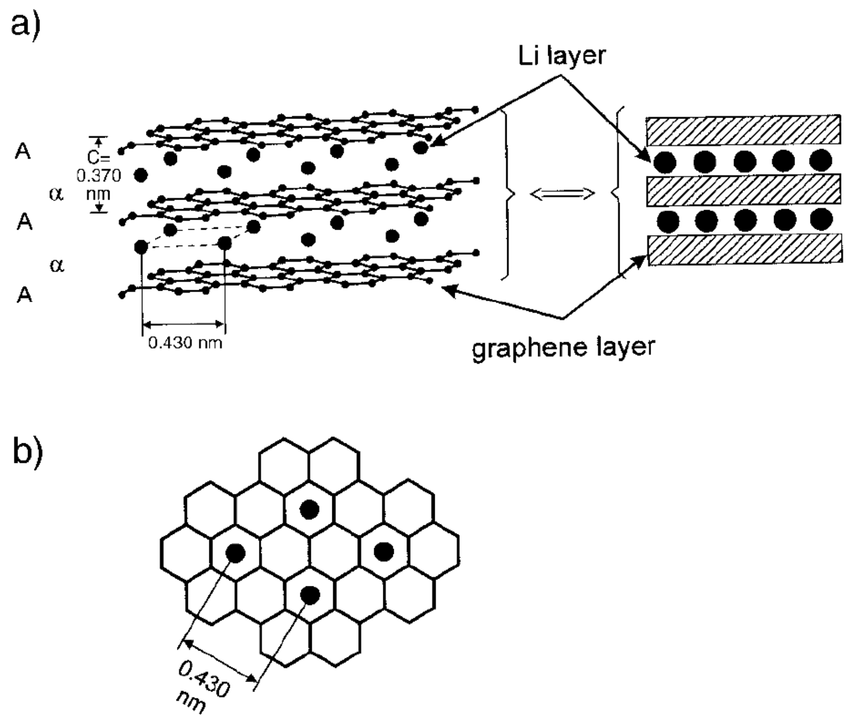

M. Winter, J. Besenhard, M. Spahr, P. Novak, Adv. Mater. 10(1998) 10

New Lithium Battery Designs - Anode

- Metallic alloy anodes
- Metal + xLi → Li_xM
- x can be greater than 1
- $Li_{4.4}Si$, for example
- However, large capacity fade
- Associated with large volume change
- +400% from Si to $Li_{4.4}Si$

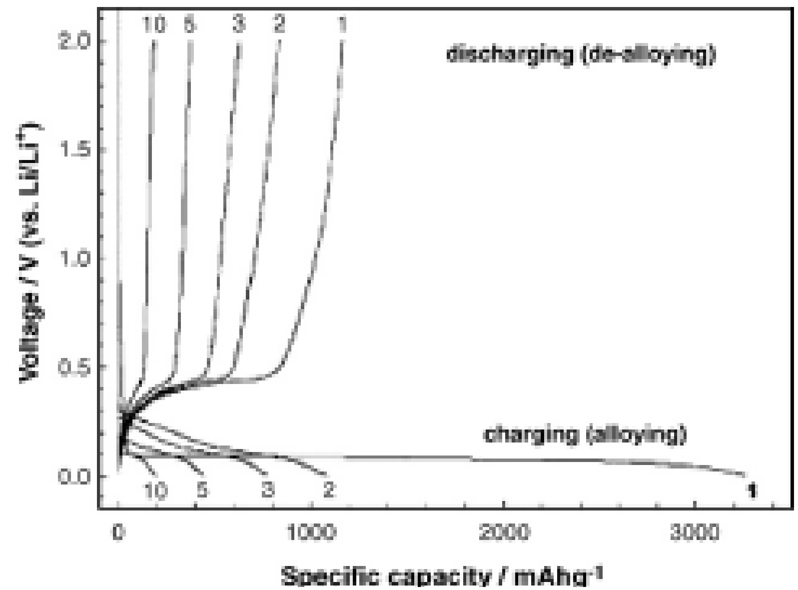

Table 1
Crystal structure, unit cell volume and volume per Si atom for the Li–Si system [10]

Compound and crystal structure	Unit cell volume ($Å^3$)	Volume per silicon atom ($Å^3$)
Silicon cubic	160.2	20.0
$Li_{12}Si_7$, ($Li_{1.71}Si$) orthorhombic	243.6	58.0
$Li_{14}Si_6$, ($Li_{1.71}Si$) rhombohedral	308.9	51.5
$Li_{13}Si_4$, ($Li_{3.25}Si$) orthorhombic	538.4	67.3
$Li_{22}Si_5$, ($Li_{4.4}Si$) cubic	659.2	82.4

A.J. Appleby, et al. J Power Sources 163(2007)1003

New Lithium Battery Designs - Anode

- Nano-structured Si
- To increase surface area
- Increase reaction rate
- Decrease volume change on intercalation

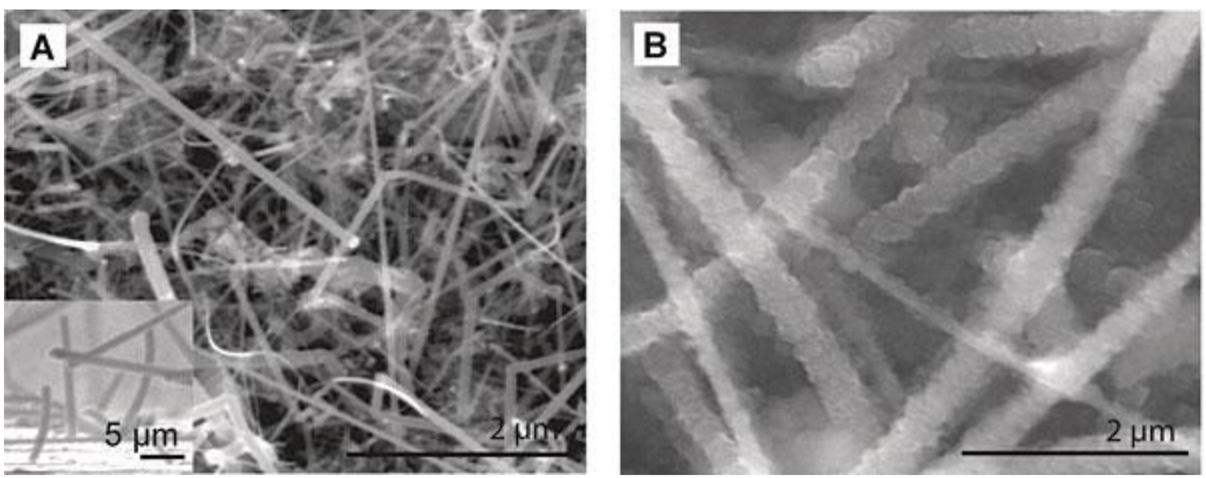

Y. Cui et al., Nature Nanotechnology 2007

Nano-Structured Si anode

- Nano-structured Si does improve cyclability
- But..cycle fade is still strong
- 1000s of cycles is a design goal

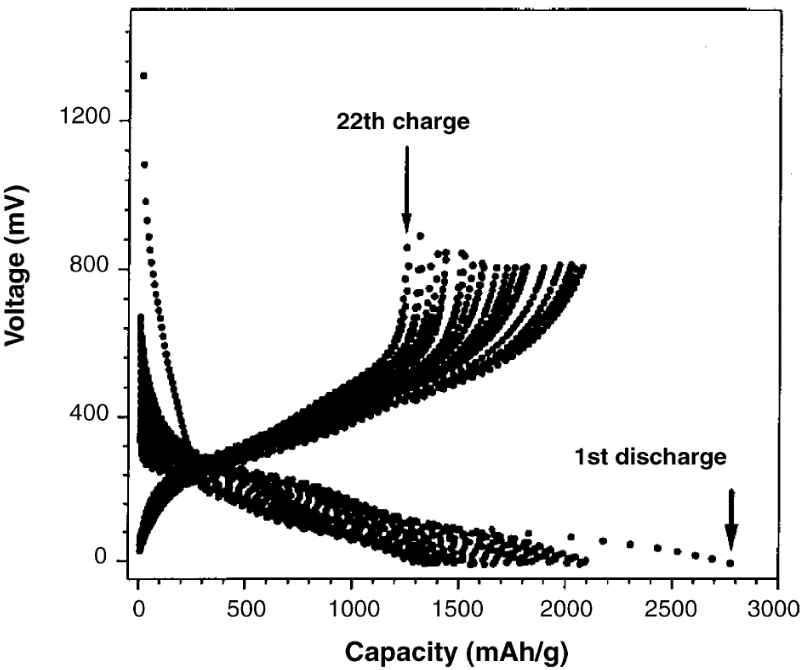

Fig. 5. §§Charge–discharge curves between 0.0 and 0.8 V at 0.1 mA cm^{-2} for nano-Si anode with 4:4:2 weight ratio of nano-Si, carbon black and PVDF binder. Electrolyte: 1 M $LiPF_6$ in ethylene carbonate (EC)–diethyl carbonate (DEC) (1:1) [22].

1 mAhr/g = 1Ahr/kg

A.J. Appleby, et al. J Power Sources 163(2007)1003

Opportunities for Improved Lithium Batteries

- Cycle life, the number of times the Lithium battery can be discharged and recharged, is often only a few hundred to at most a thousand
  - This leads to lifetimes of only a year or two
- Unbroken paradigm of good cyclability and low Lithium capacity (activity) at the anode
  - Li metal has the highest activity, but the poorest cyclability
  - Li-C has low activity, Li_6C, but among the highest cyclability
- New materials are needed that can help break this paradigm of low capacity (activity), but good cyclability

New Anodes for Lithium Batteries

- How can we store more Li at near unit activity, but safely, reversibly, and cheaply?
- Li readily alloys with many metals
  - Li-Si, Li-Ge, Li-Al…
  - However, large volume changes often occur (> 100 %) with these alloy reactions
  - Anode cracks and crumbles after only a few cycles
- Can we create these Li-alloys inside a buffering material that will accommodate the volume changes leading to improved cyclability, but maintain Lithium activity, hence high voltage and energy density?

New Anodes for Lithium Batteries

- Needed: An Anode Material which:
  - Conducts Li^+ ions rapidly to insure fast electrode kinetics and charge transfer
  - Has significant fractions of alloying metal, such as Si or Ge, to store large amounts of Li to insure high Li activity and cell voltage
  - Has a relatively low mechanical modulus that will accommodate volume changes during alloying reactions
  - Is chemically stable under highly reducing conditions of the Lithium battery anode
  - Relatively cheap, plentiful, and easily manufactured

Glasses as High Capacity, High Voltage, High Cyclability, Safe Lithium Battery Anodes

- Idea: Li^+ ion conducting chalcogenide glass anodes
  - Chalcogenide glasses are among the highest of all Li^+ ion conductors known, 10^{-3} $(\Omega cm)^{-1}$ at 25^oC
  - Chalcogenide glasses can be readily made using Si and Ge over a continuous range of compositions, ~50 at% to ~ 10 at%
  - Chalcogenide glasses are significantly "softer" than oxide glasses, MPa moduli versus GPa, for example
  - Sulfide glasses while commonly unstable under oxidizing conditions can be quite stable under reducing conditions
  - Due to their ease of preparation, glasses can be inexpensively prepared, especially in powder form, using mechanical milling where no melting is required

Inorganic Glasses as Hosts for Active Materials

- Sulfide glasses show significantly higher Li^+ ion conductivity over their oxide counterparts
  - $Li_2O + P_2O_5$ has $\sigma_{RT} \sim 10^{-9}$ (S/cm)
  - $Li_2S + P_2S_5$ has $\sigma_{RT} \sim 10^{-3}$ (S/cm)
  - Perhaps sulfide glasses might serve as high capacity anodes?

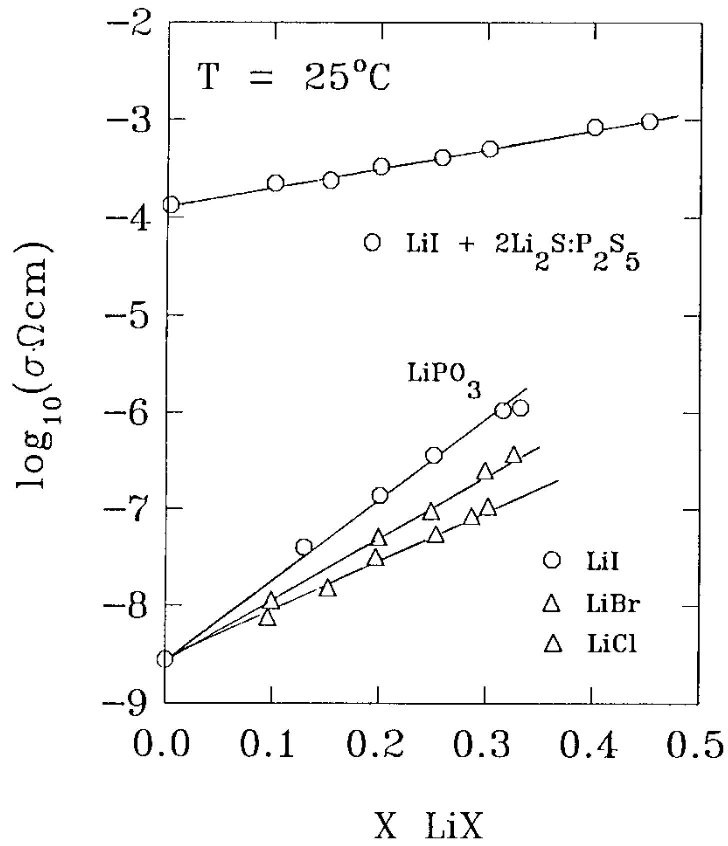

S.W. Martin JACerS 74(1991)1767

Comparative behavior of pure Ge

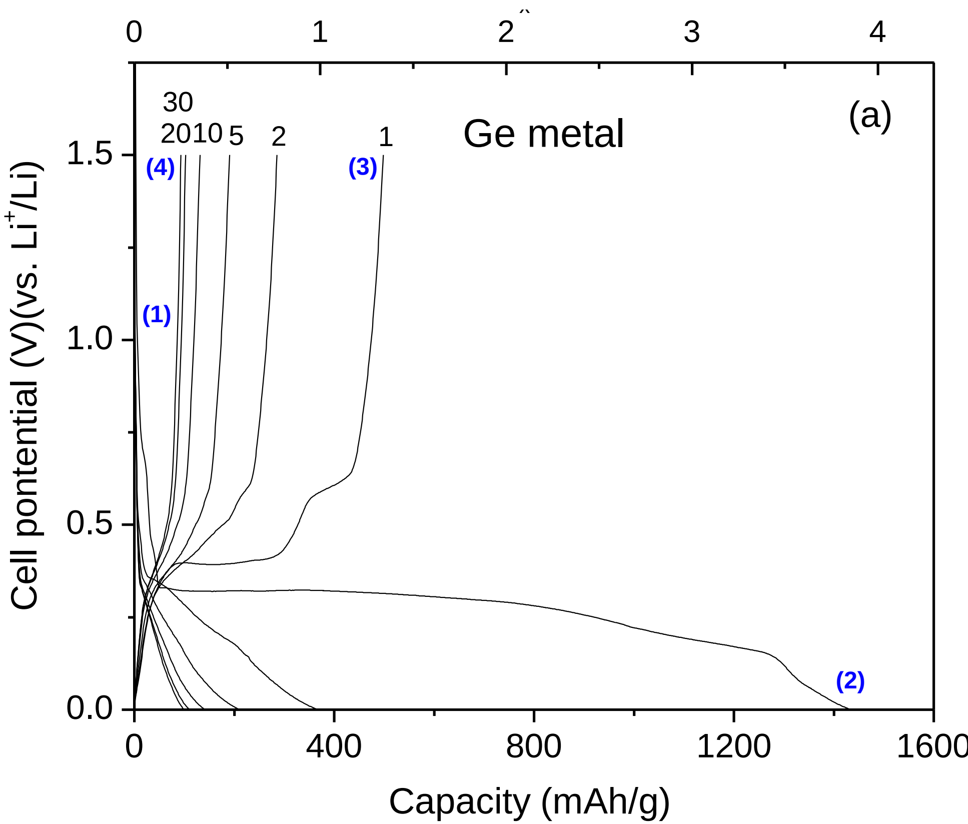

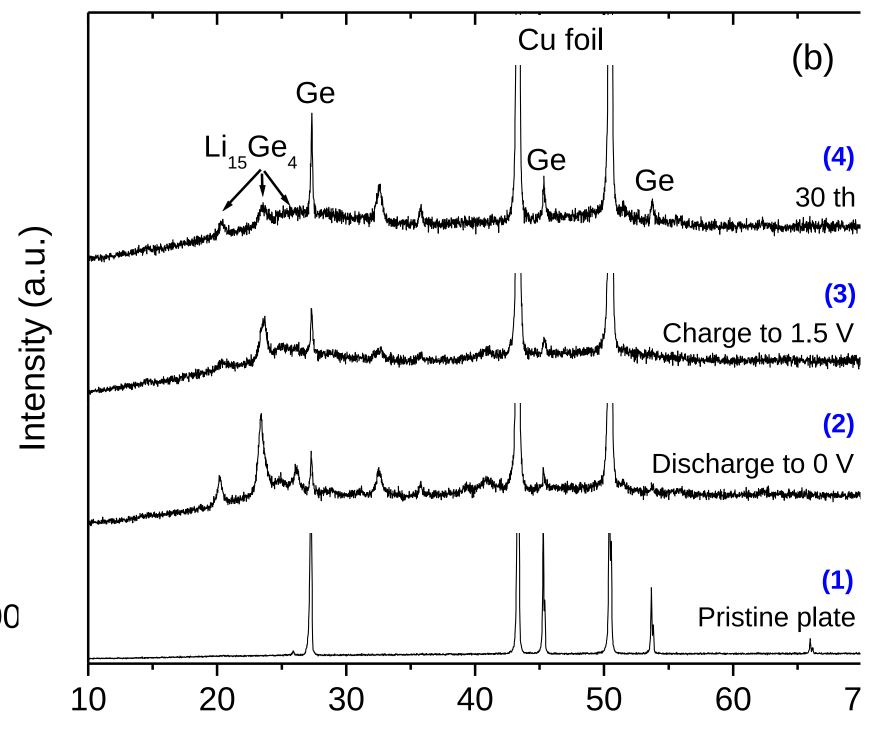

Comparative behavior of GeO_2 Glass

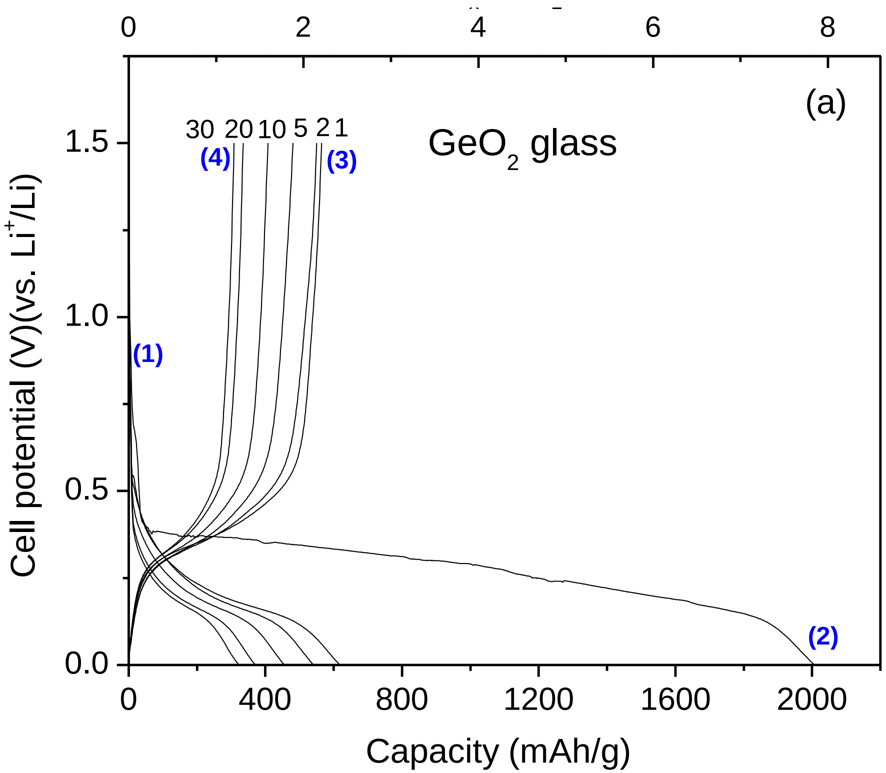

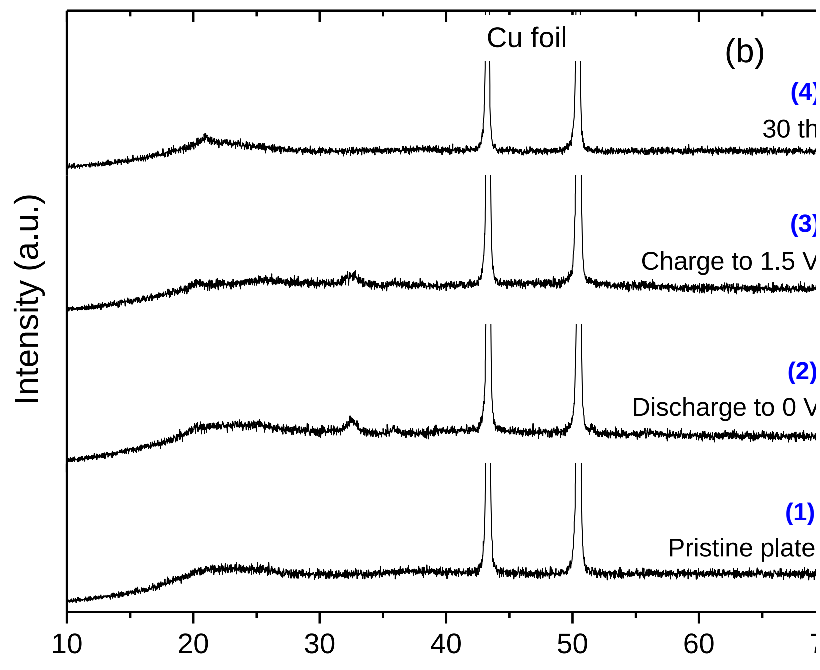

GeS_2 Glass Li anodes

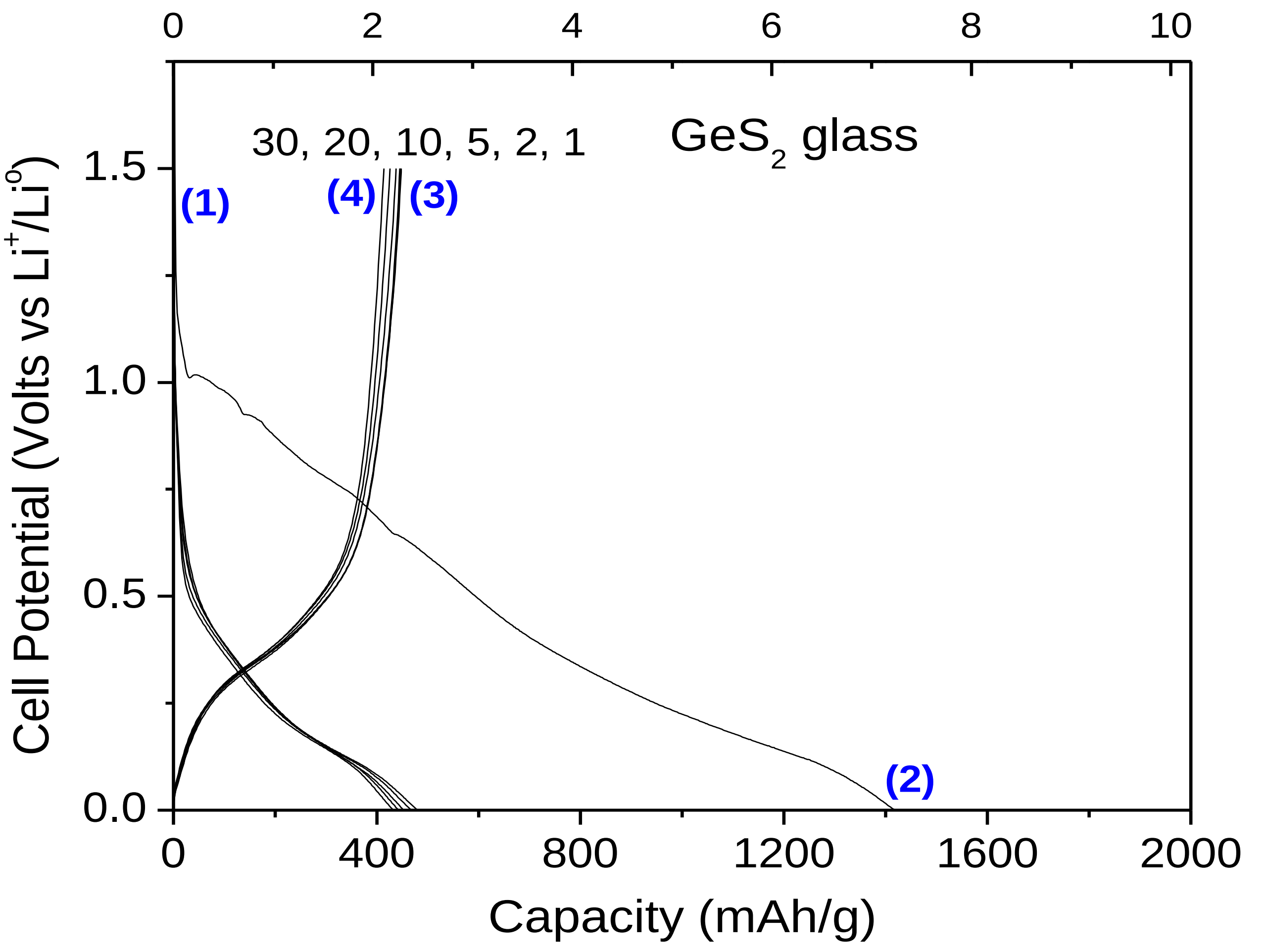

Ge-based Active Material Anodes

- GeS_2 glass based anode has best reversibility

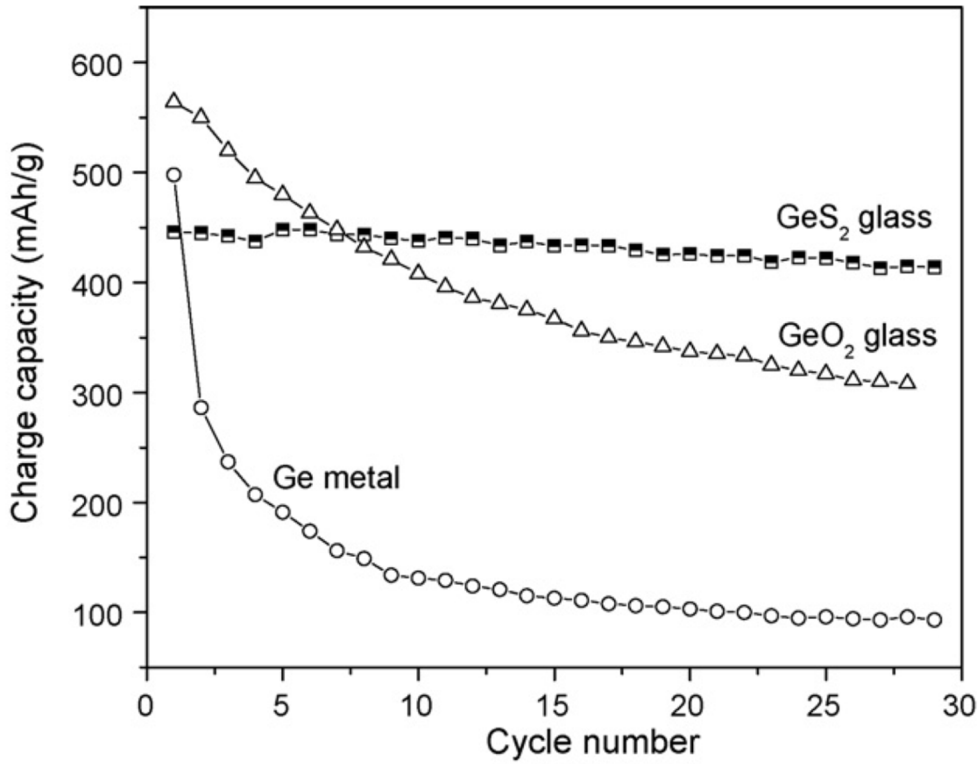

Fig. 5. Cycle-life performance of Ge metal, GeO_2 glass, and GeS_2 glass, respectively. They are operated between 1.5 and 0 V at the rate of 0.1 C.

Kim and Martin et al. Electrochimica Acta 53(2008) 5058

Plausible mechanism of Glassy Anodes

- Reaction steps:

$$x/2GeS_2 + 2xLi \rightarrow xLi_2S + x/2Ge$$

$$Ge + nLi \rightarrow Li_nGe$$

Components of Li-ion Batteries

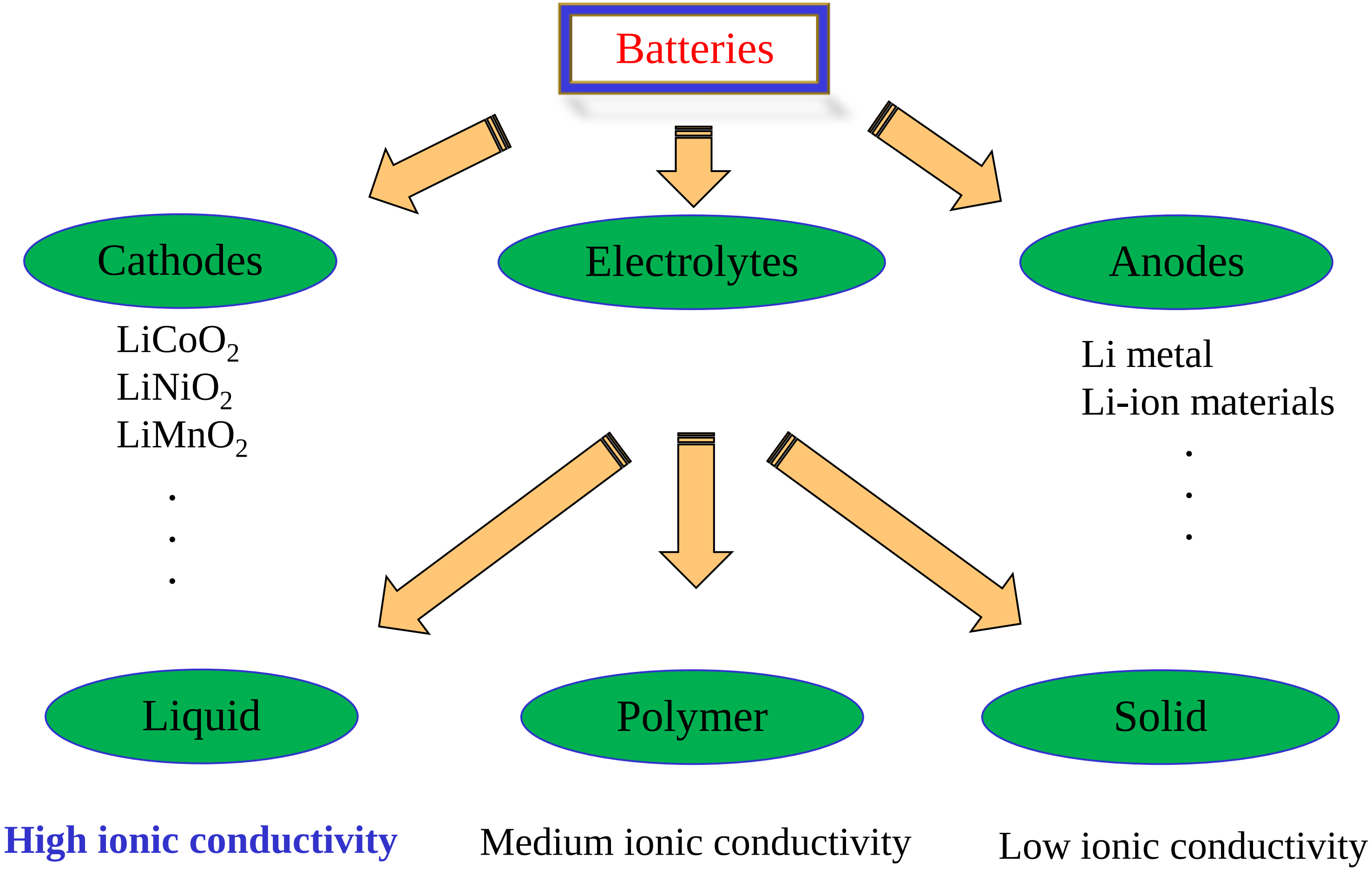

Li-Battery Anode and Cathode Combinations

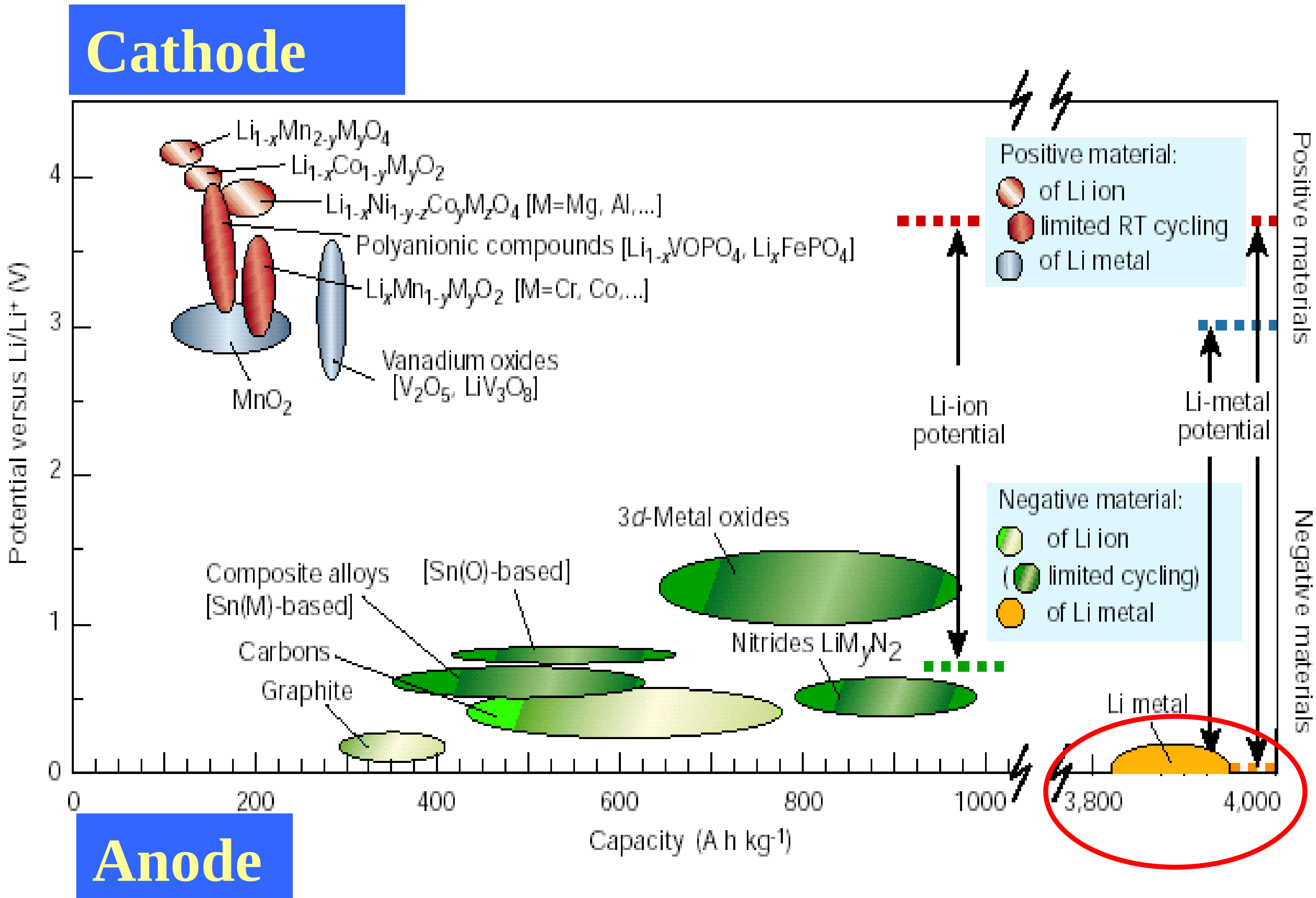

J.M. Tarascon, M. Armand, Nature, 414, 15 (2001) 359

Lithium Dendrite Formation in Lithium Batteries

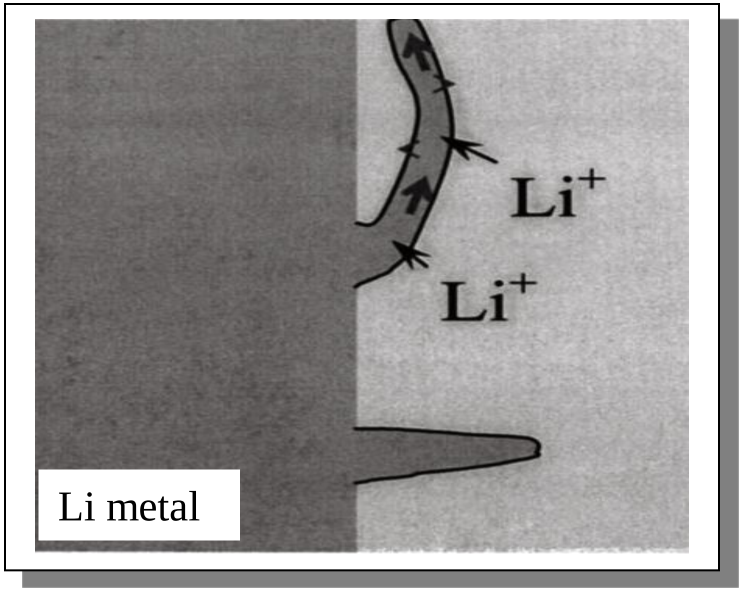

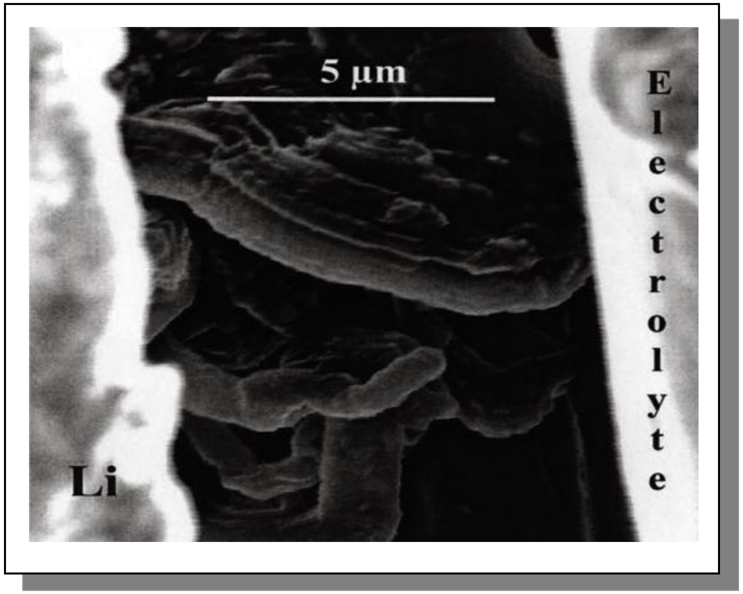

- Non-epitaxial deposition of lithium after each cycle leads to the growth of uneven "fingers" or dendrites
- Internal connection results in short circuits in the battery

M. Dolle et al. Electrochemical and Solid-State Letters, 5(12) (2002)A286

Components of Li-ion Battery

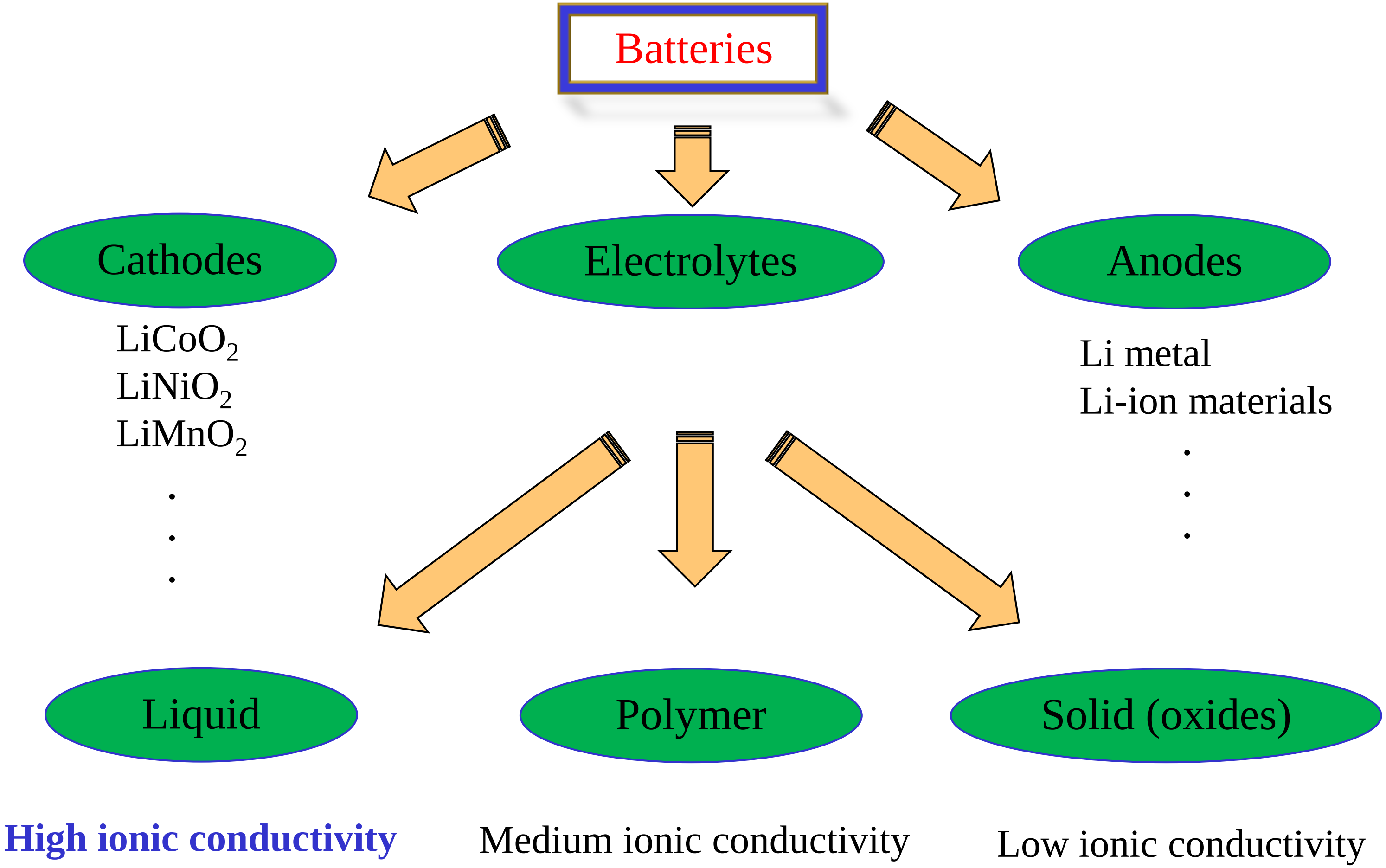

Advantages of Solid State Thin Film Batteries

- High power and energy densities
  (Li metal as an anode material)

- Various sizes (thickness and area to optimized capacity)

- Wide operating temperatures (between -40 ^{o}C and 150 ^{o}C)
  (Low temperature dependence)

- No liquid components
  (No leakage problem)

- High cyclability
  (Reversability over many charge and discharge cycles)

LiPON (Li_3PO_4 sputtered in N_2) Thin Film Battery

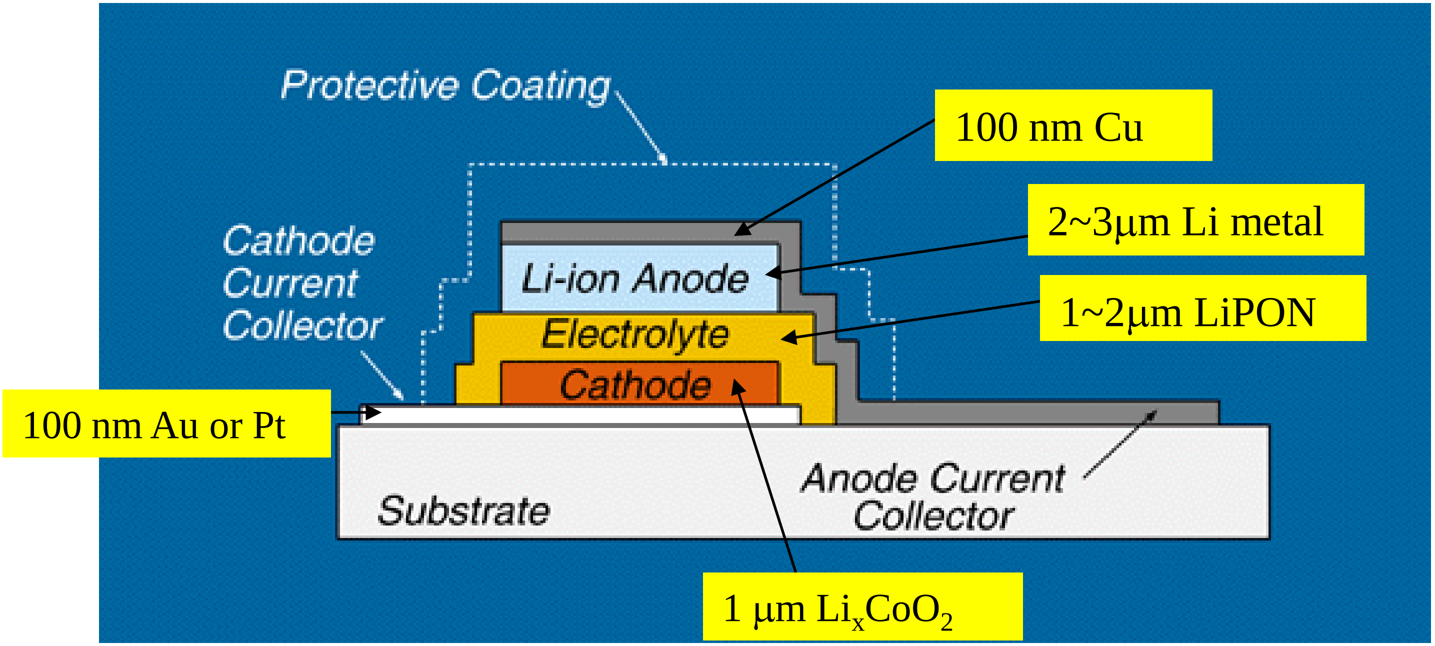

- Long term stability with lithium metal
- Good stability in air
- Easy preparation and characterization
- Relatively low ionic conductivity, ~ 10^{-6} (S/cm) at 25 °C

J.B. Bates, N. J. Dudney, et al. Solid State Ionics 135(2000)33

Materials Selection

Sulfide materials show high ionic conductivity

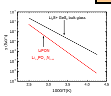

B_2S_3, SiS_2, Li_2S, GeS_2, P_2S_5....

n = 1	$1Li_2S + GeS_2$	$0.5Li_2S + 0.5GeS_2$	Li_2GeS_3
n = 2	$2Li_2S + GeS_2$	$0.67Li_2S + 0.33GeS_2$	Li_4GeS_4
n = 3	$3Li_2S + GeS_2$	$0.75Li_2S + 0.25GeS_2$	Li_6GeS_5

(Ar atmosphere)

Lithium thio-germanate thin film electrolytes

Experimental Methods

- Introduction
- Experimental Methods
- Results and Discussion
  - Surface and structural characterization by XRD, IR and Raman
  - Compositional characterization by XPS
  - Ionic conductivity measurement by impedance spectroscopy
- Conclusions and Future Work

RF Magnetron Sputtering System

RF Magnetron Sputtering System

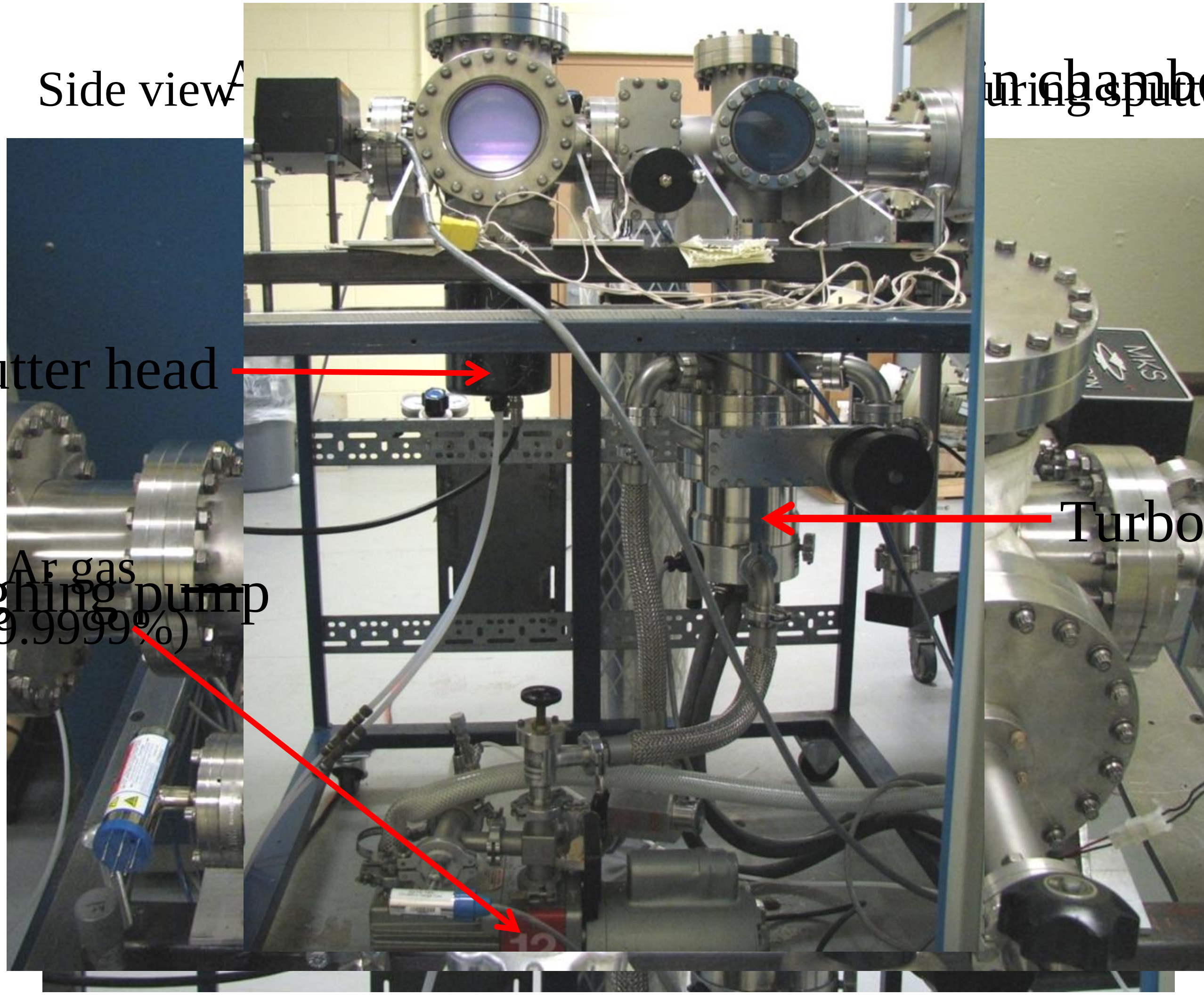

Target Preparation

- Commercial source for Li_2S – (Alfa, 99.9%)
- Ge + 2S → GeS_2 – Sealed SiO_2 tube

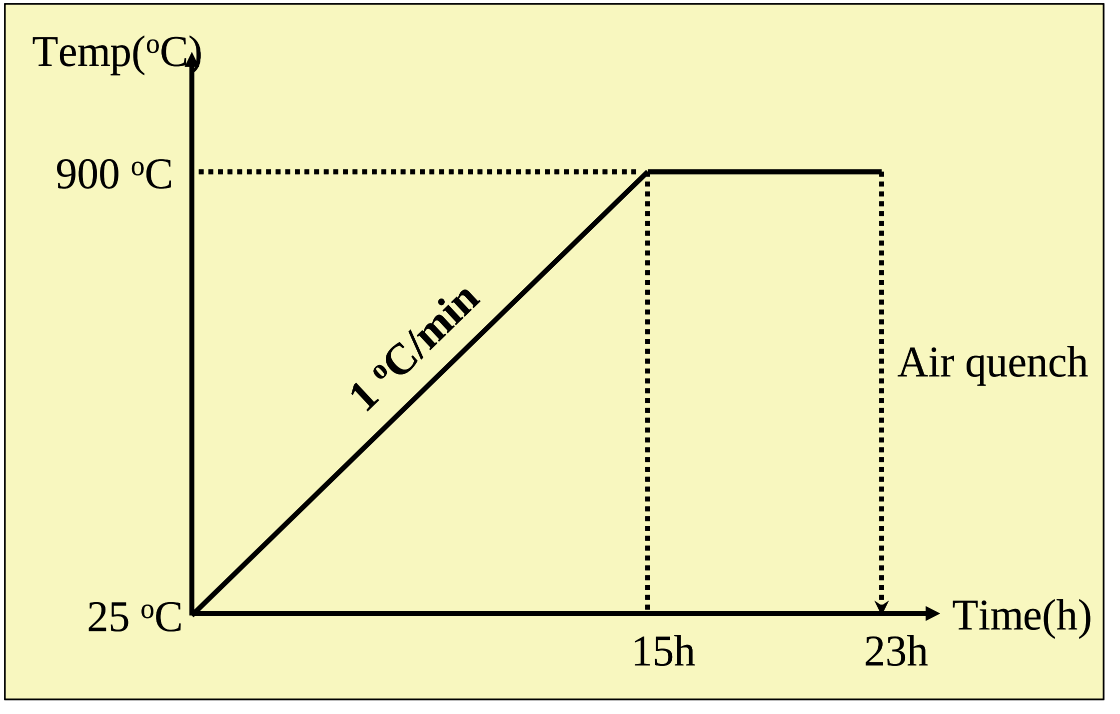

Target Preparation

- nLi_2S+GeS_2 (n=1, 2 and 3)→ 950 ^{o}C for 15 min.

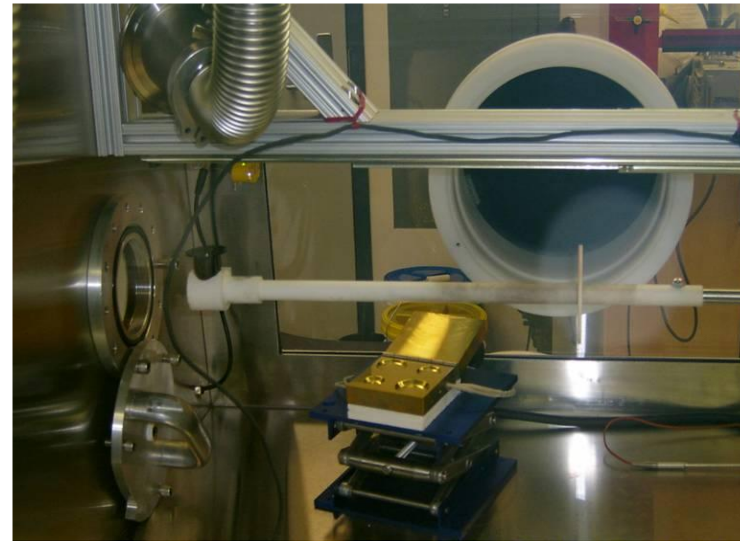

- Melted target materials were quenched onto a brass plate
- Quenched materials were milled using Spex milling to make powder

- Pressed using 2” stainless steel die set
- Loaded with 30,000 lbs overnight

Target Preparation

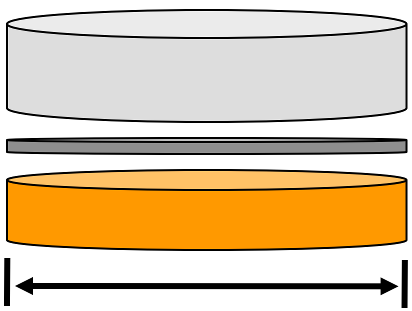

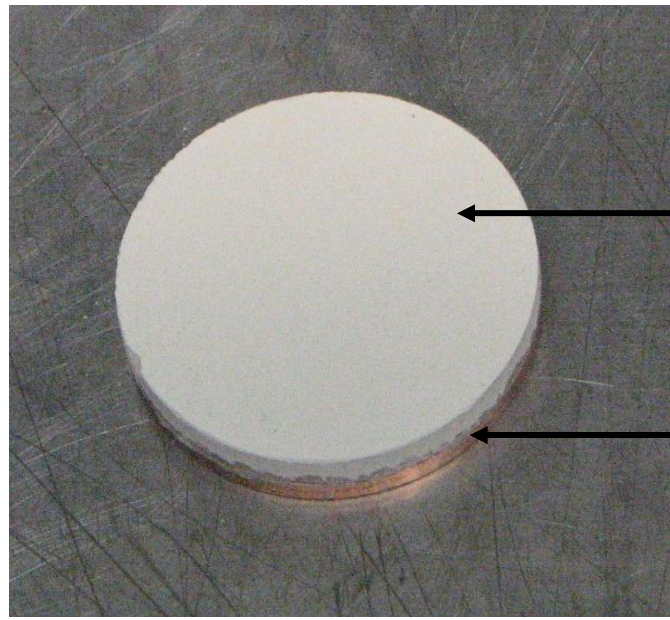

Targets are attached onto a copper plate by silver paste

Sputtering Conditions

- The pressure for sputtering : 30mtorr
- Sputtering power : 50 W
- Ar gas atmosphere (N_2 in future work)

nLi_2S+GeS_2 target with Ar atmosphere

Results and Discussion

- Introduction
- Experimental Methods
- Results and Discussion
  - Surface and structural characterization by SEM, Raman and IR
  - Compositional characterization by XPS
  - Ionic conductivity measurement by impedance spectroscopy
- Conclusions and Future Work

The Outline of the Characterizations

Materials	Structure				Composition	Ionic Conductivity
	SEM	XRD	Raman	IR	XPS	Impedance spectroscopy
Starting materials Li_2S GeS_2		✓	✓	✓		
Targets Li_2GeS_3 Li_4GeS_4 Li_6GeS_5		✓	✓	✓	✓	
Thin films Li_2GeS_3 Li_4GeS_4 Li_6GeS_5	✓		✓	✓	✓	✓

Surface Morphology and Thickness of the Thin Film

Li_4GeS_4 thin film in Ar atmosphere

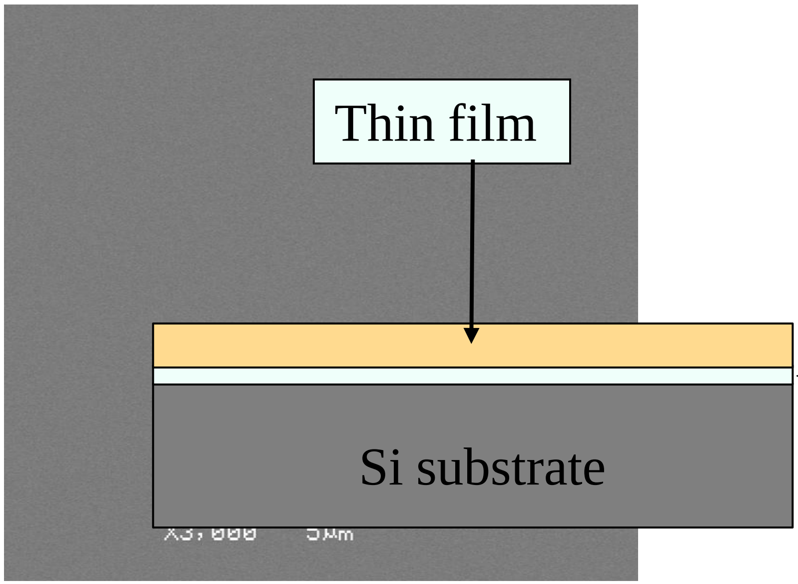

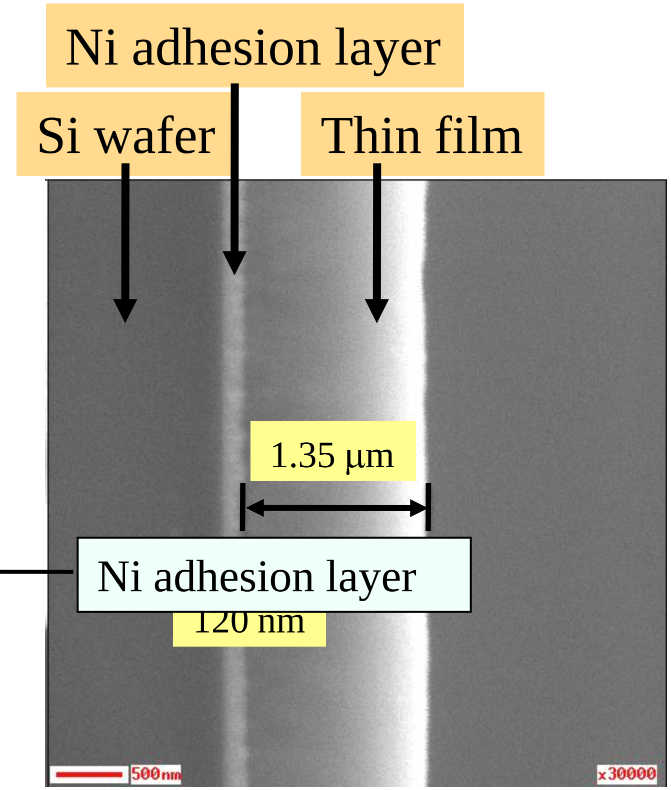

- No cracks or pits that increase contact resistance between electrodes and electrolytes

- Sputtering time : 4 hours
- Sputtering rate : 1.35 μm/4h ≈ 6 nm/min.
- Sputtering power : 50 W@ 30 mtorr

XRD Data of the Starting Materials

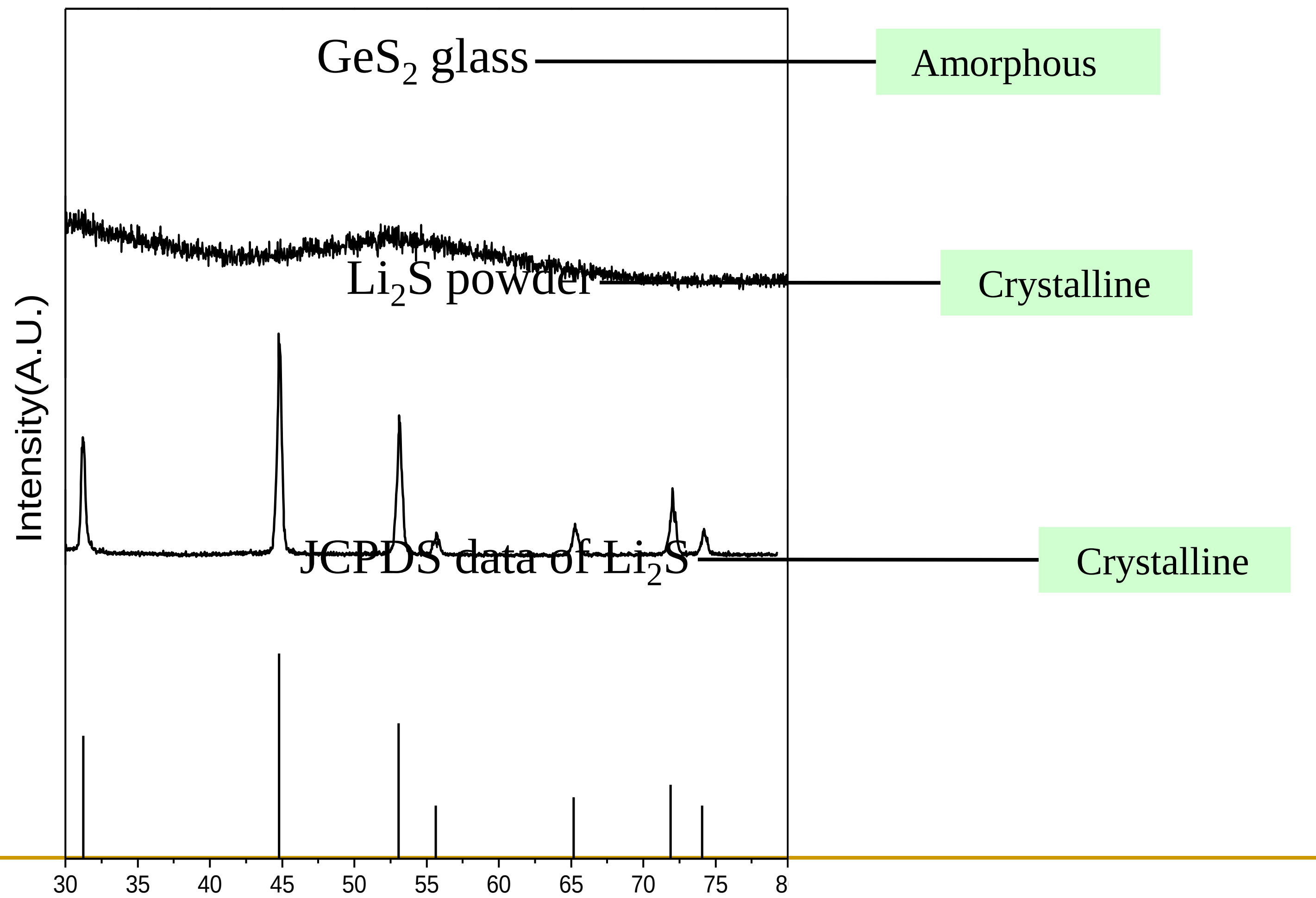

XRD Data of the Target Materials

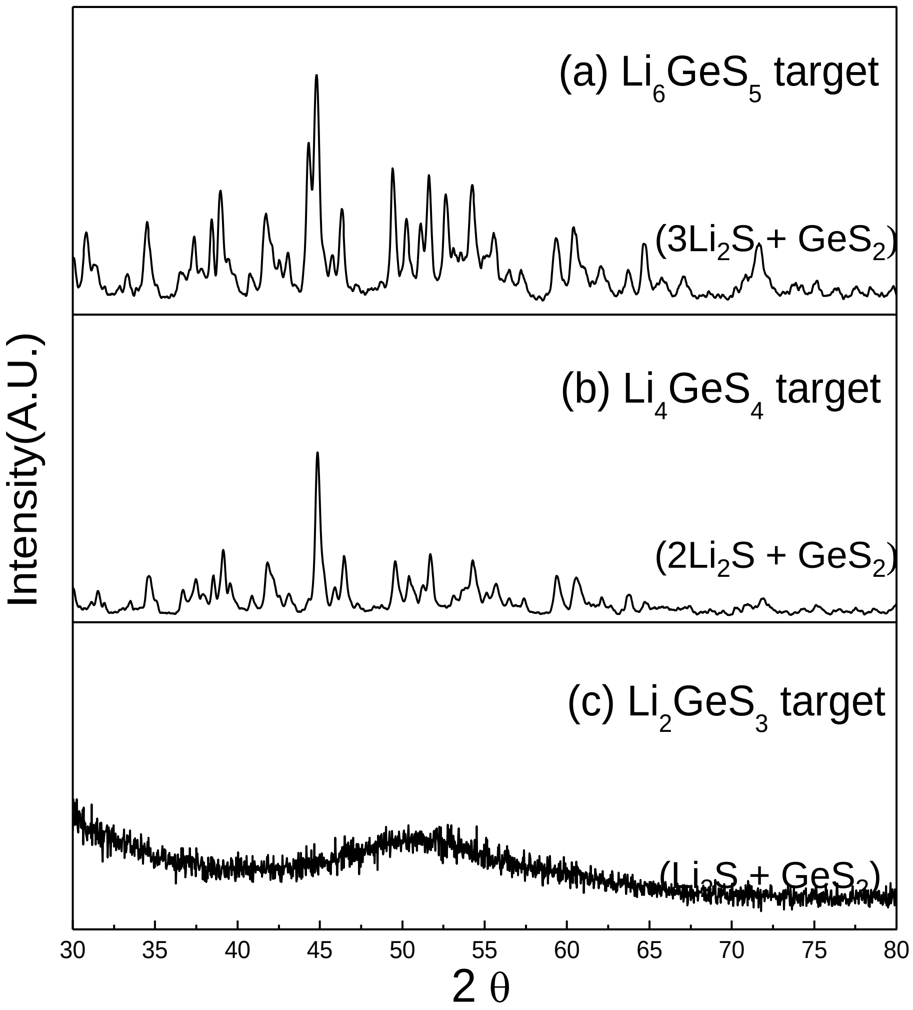

- (a) Li_6GeS_5 target – polycrystalline
- (b) Li_4GeS_4 target – polycrystalline
- (c) Li_2GeS_3 target – amorphous

XRD Data of the Target Materials

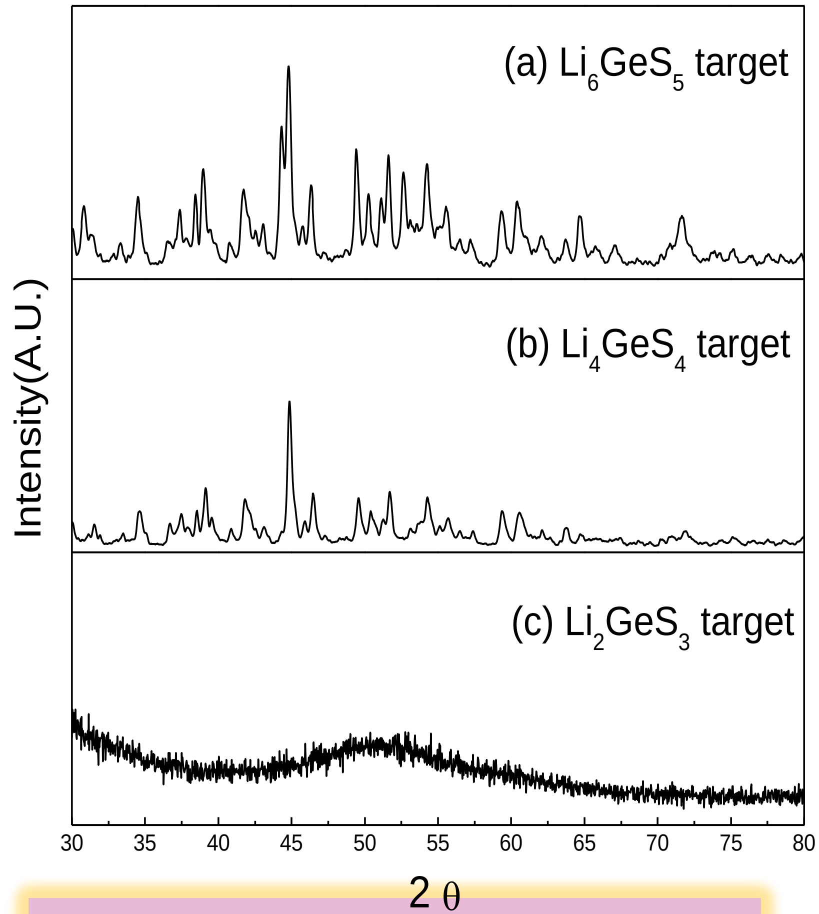

- (a) Li_6GeS_5 target – polycrystalline
- (b) Li_4GeS_4 target – polycrystalline
- (c) Li_2GeS_3 target – amorphous

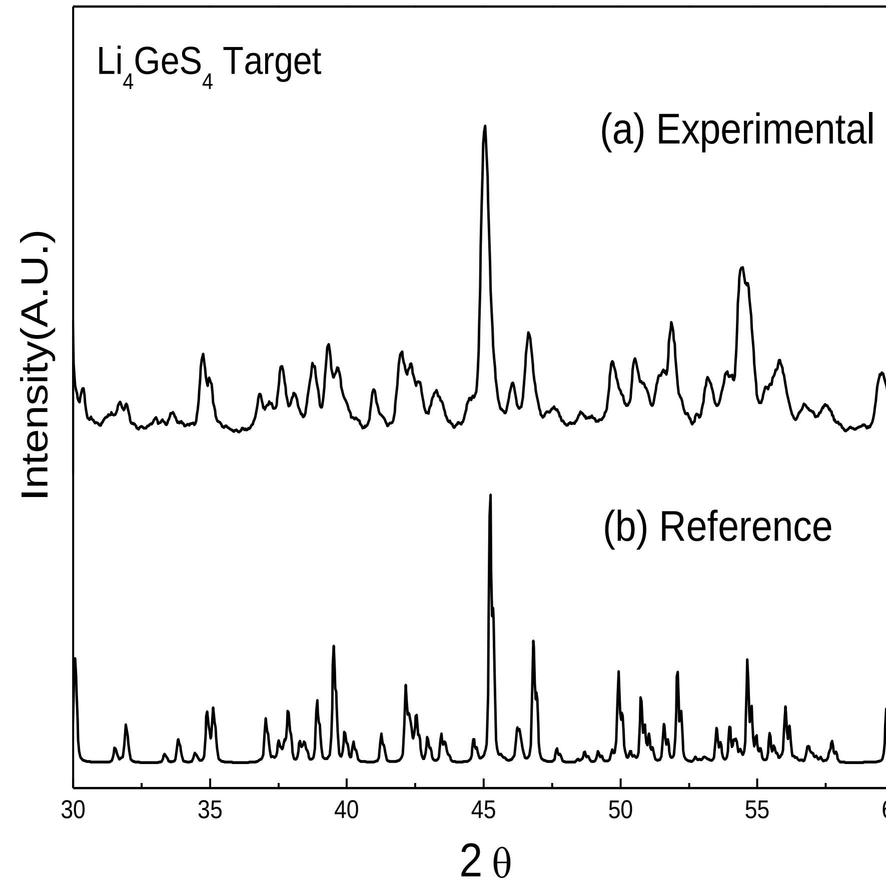

R. Komiya et al., Solid State Ionics 140 (2001) 83.

- (a) Li_4GeS_4 target – polycrystalline
- (b) Li_4GeS_4 literature data – crystalline

Raman Spectra of the Starting Materials

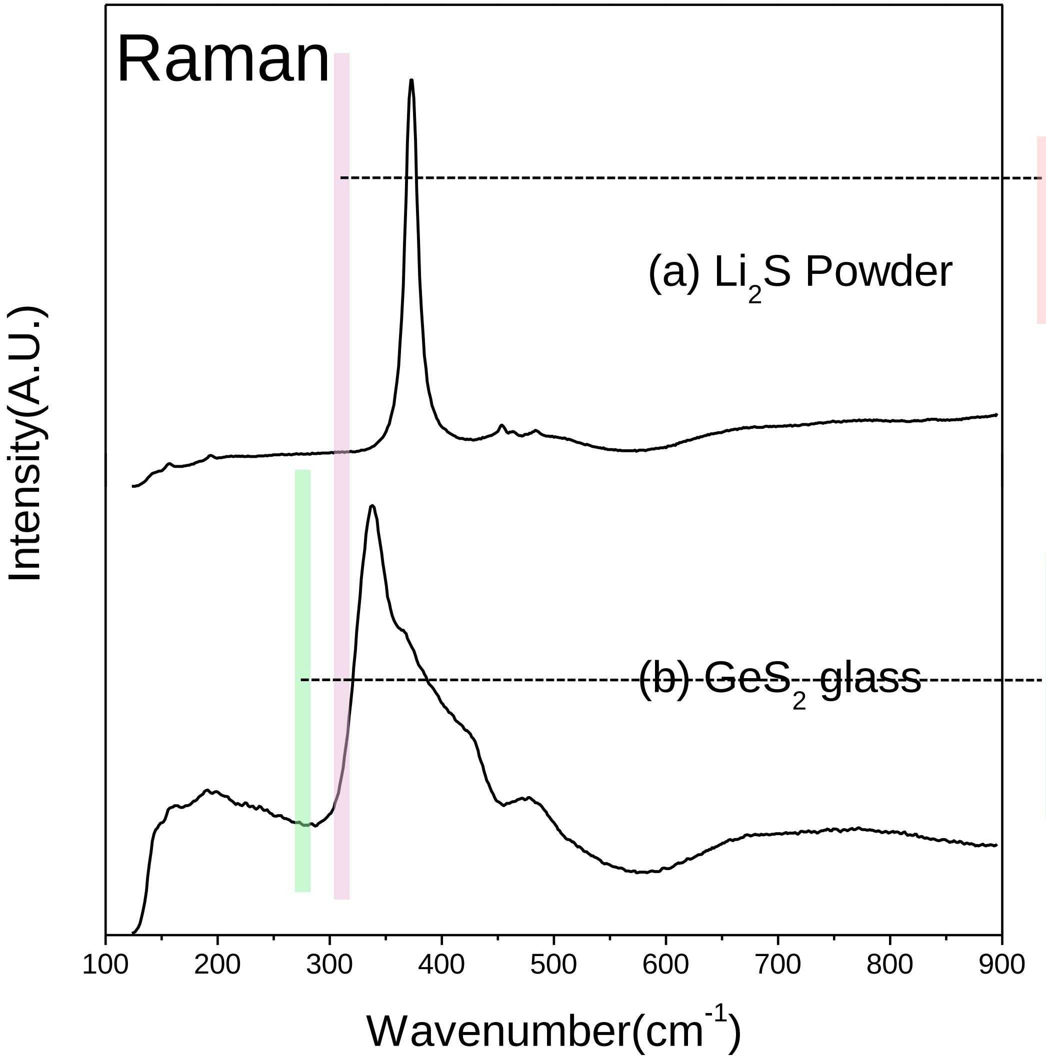

~ 375 cm^{-1}
assigned to Li^+S^-

~ 340 cm^{-1}
assigned to Ge-S-Ge
(Bridging Sulfur)

Raman Spectra of the Target Materials

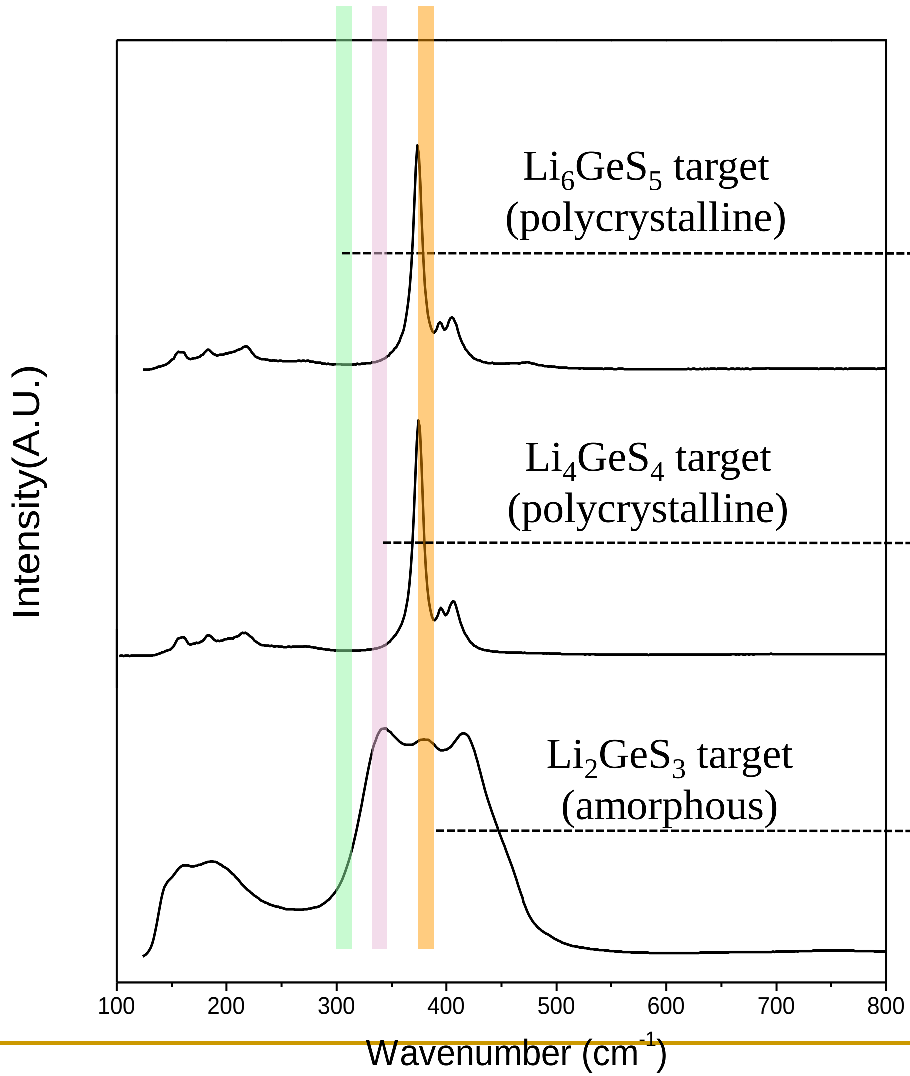

~ 340 cm^{-1} assigned to Ge-S-Ge (Bridging Sulfur)

~ 375 cm^{-1} assigned to Li^+S^-

~ 415 cm^{-1} assigned to Ge-S^- (Non-bridging sulfur)

Raman Spectra of the Thin Films

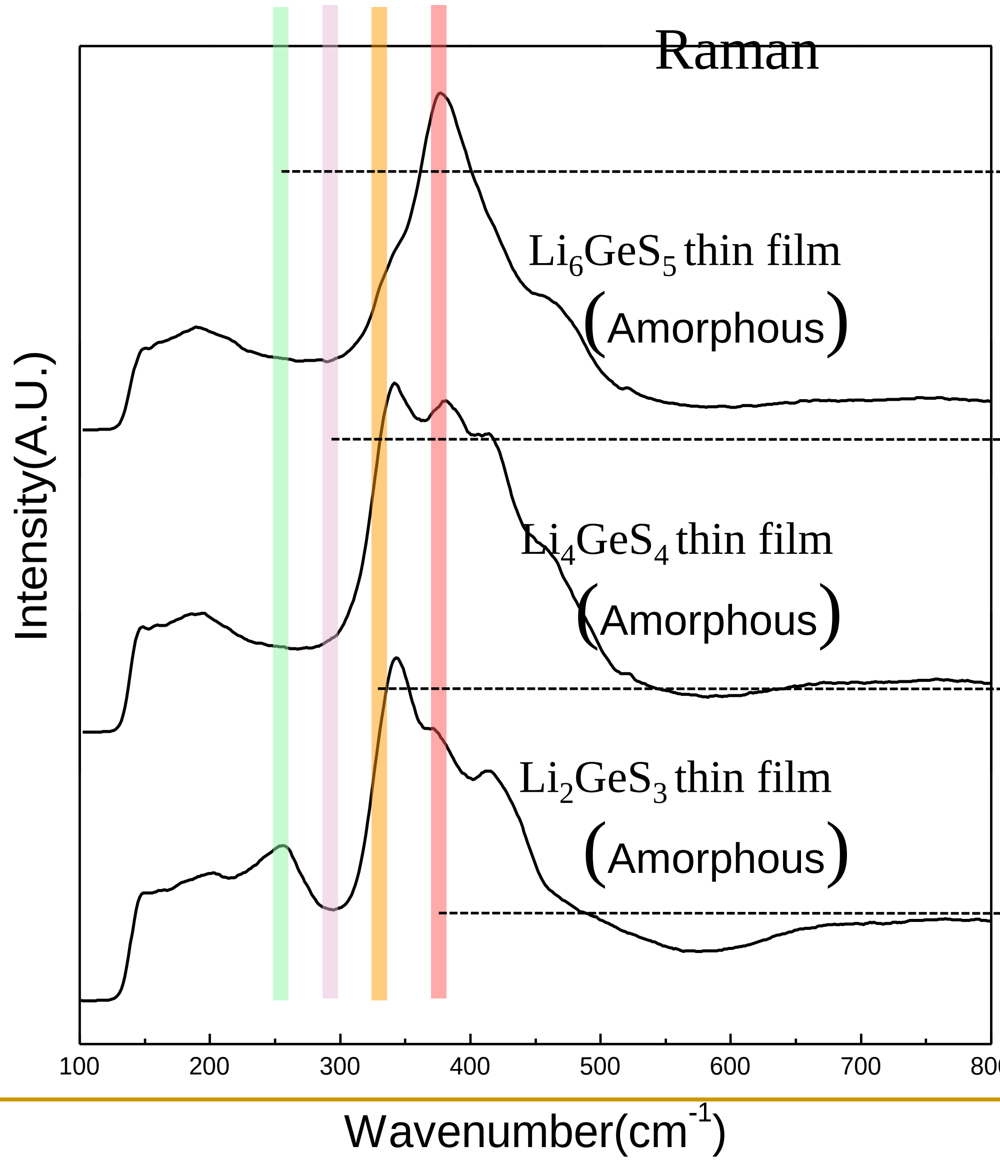

~ 340 cm^{-1} assigned to
Ge-S-Ge
(Bridging Sulfur)

~ 375 cm^{-1} assigned to
Li^+S^-

~ 415 cm^{-1} assigned to
$Ge\text{-}S^-$
(Non-bridging sulfur)

~ 460 cm^{-1} assigned to
$Ge\text{-}S^-$
(Non-bridging sulfur)

Raman Spectra of the Starting, Target Materials, Thin Films

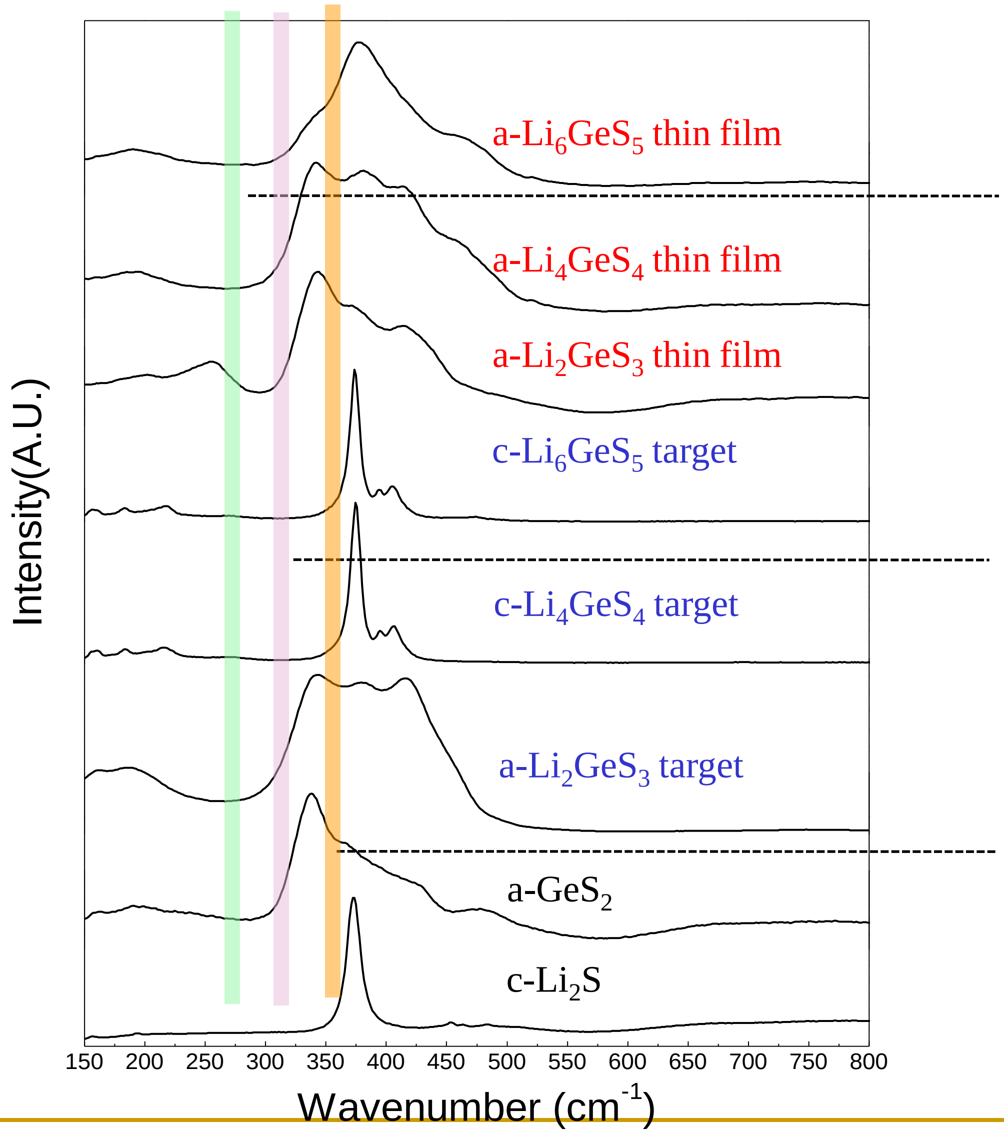

~ 340 cm^{-1} assigned to Ge-S-Ge (Bridging Sulfur)

~ 375 cm^{-1} assigned to Li^+S^-

~ 415 cm^{-1} assigned to $Ge\text{-}S^-$ (Non-bridging sulfur)

XPS Compositional Data of the Starting Materials

	Li1s (0.028)	S2 (0.7
Li_2S	44.7	22
	66.1	33
	66.7	33

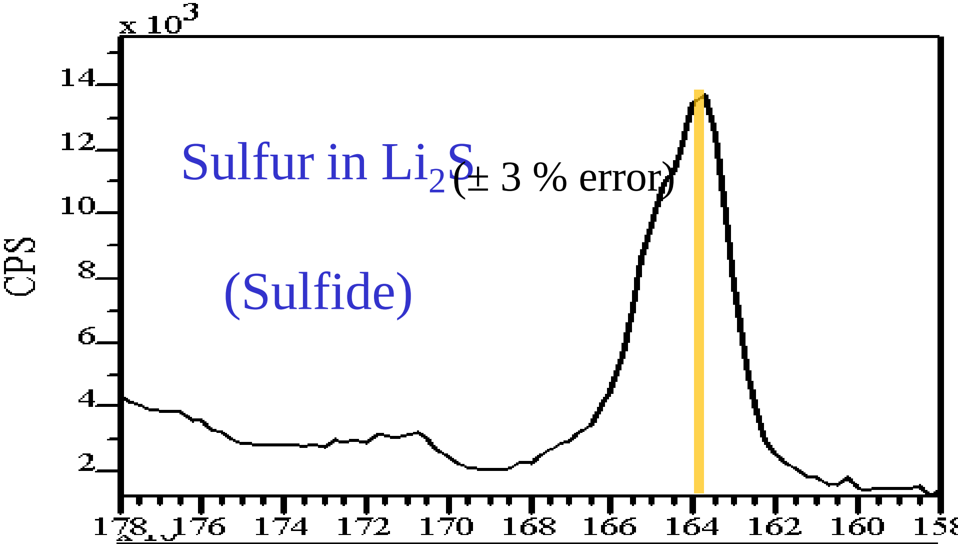

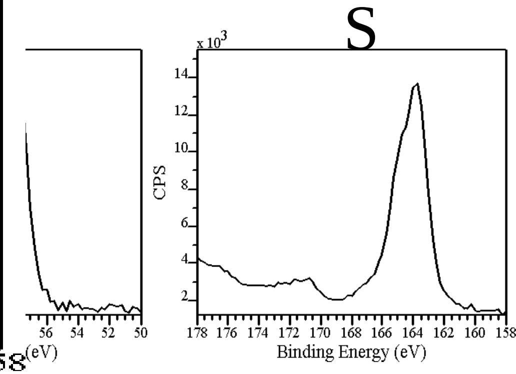

	Ge2p3 (5.400)	S2 (0.7
GeS_2	34.2	59.
	36.7	63.
	33.3	66.

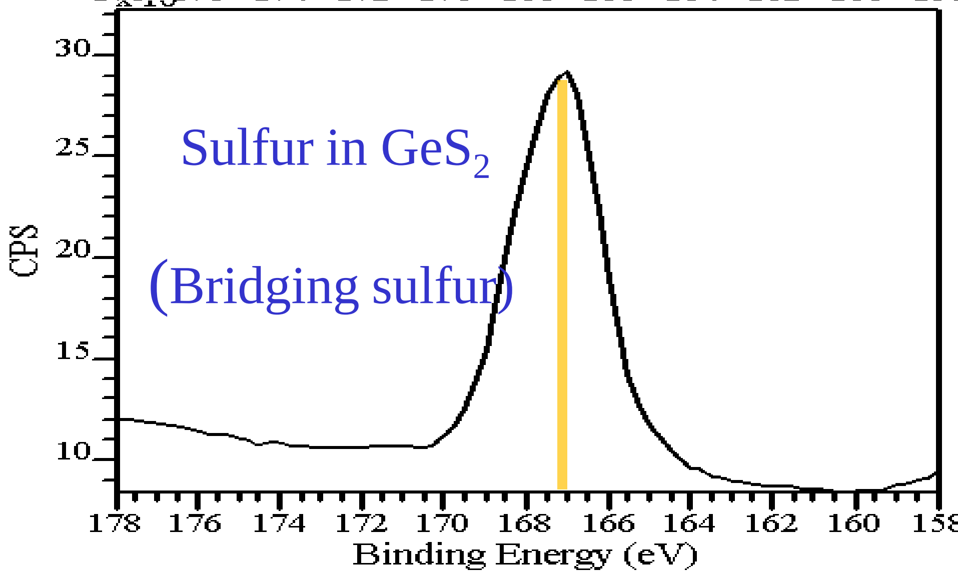

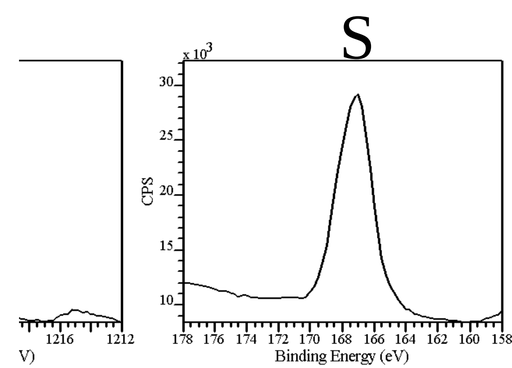

Deconvoluted S2p Core Peaks of the Starting Materials

- Deconvoluted S2p core peaks for Li_2S

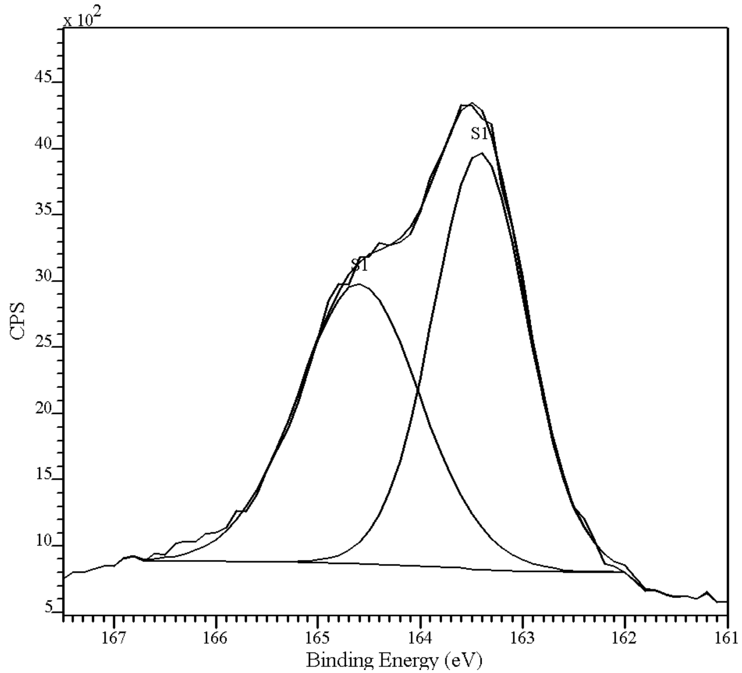

- One doublet
- 100 % Sulfide

- Deconvoluted S2p core peaks for GeS_2

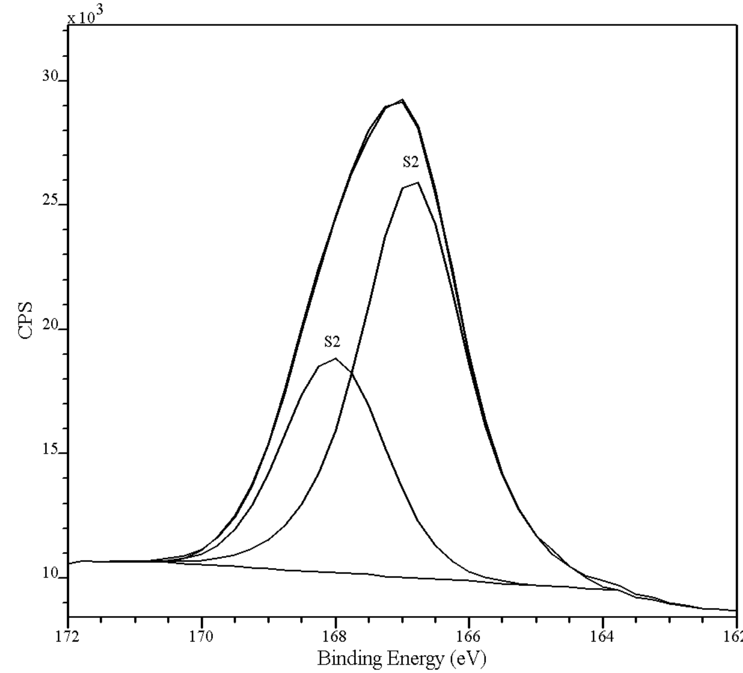

- One doublet
- 100 % Bridging sulfur

XPS Compositional Data of the Target Materials

	Li 1s (0.028)	Ge 2p3 (5.400)	S 2p (0.717)	C 1s (0.314)	O 1s (0.733)	Comments (Sensitivity factor)
Li_2GeS_3 target (n=1)	26.1	16.4	41.3	10.3	5.9	(± 3 %) As prepared
	31.1	**19.5**	**49.4**	**-**	**-**	**Ignore C and O**
	33.3	16.7	50.0	0	0	Theoretical values

	Li 1s (0.028)	Ge 2p3 (5.400)	S 2p (0.717)	C 1s (0.314)	O 1s (0.733)	Comments (Sensitivity factor)
Li_4GeS_4 target (n=2)	36.5	9.6	40.2	8.6	5.1	As prepared
	42.3	**11.1**	**46.6**	**-**	**-**	**Ignore C and O**
	44.4	11.2	44.4	0.0	0.0	Theoretical values

	Li 1s (0.028)	Ge 2p3 (5.400)	S 2p (0.717)	C 1s (0.314)	O 1s (0.733)	Comments (Sensitivity factor)
Li_6GeS_5 target (n=3)	40.4	8.0	37.2	6.5	7.9	As prepared
	47.2	**9.3**	**43.5**	**-**	**-**	**Ignore C and O**
	50.0	8.3	41.7	0	0	Theoretical values

XPS S2p Core Peaks of the Li_2GeS_3 Target Material

E_b $S2p_{3/2-1/2}$	Experimental ratio	Theoretical ratio
160.7 – 161.9	NBS (64.5 %)	NBS (66.7 %)
161.7 – 162.9	BS (35.5 %)	BS (33.3 %)

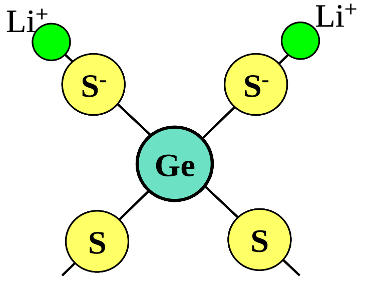

$Li_2GeS_{2/2}S_2$

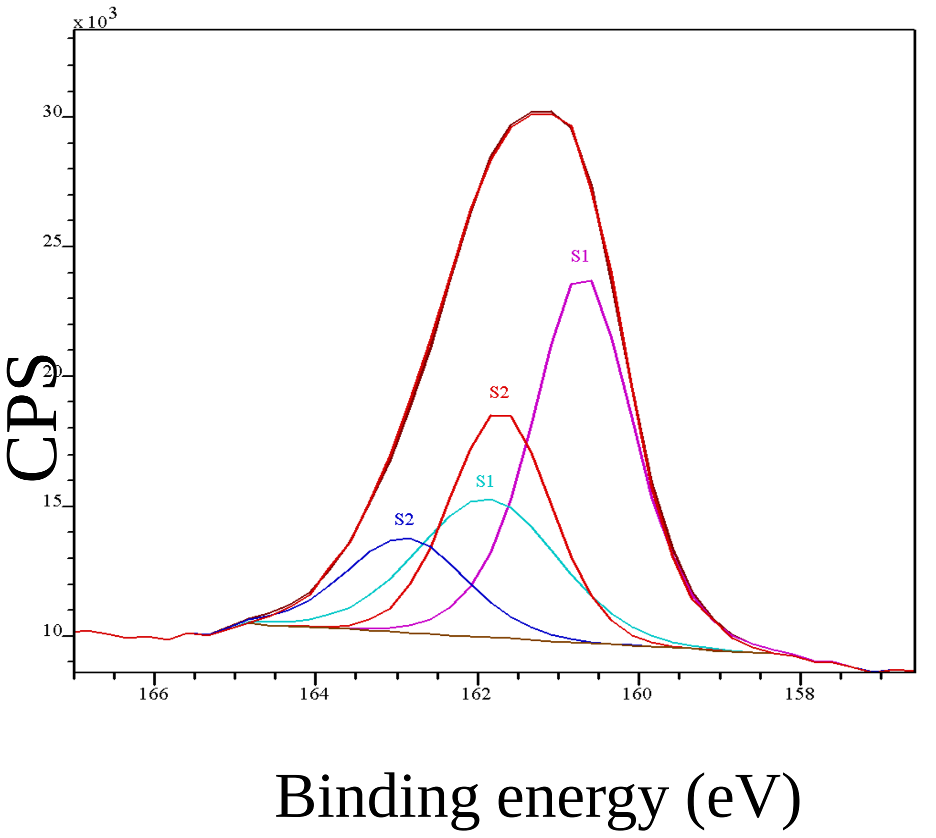

XPS S2p Core Peaks of the Li_4GeS_4 Target Material

E_b $S2p_{3/2-1/2}$	Experimental ratio	Theoretical ratio
161.0 – 162.2	NBS (92.2 %)	NBS (100 %)
161.9 – 163.1	BS (7.8 %)	BS (0 %)

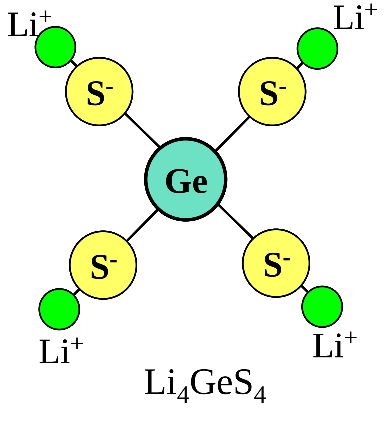

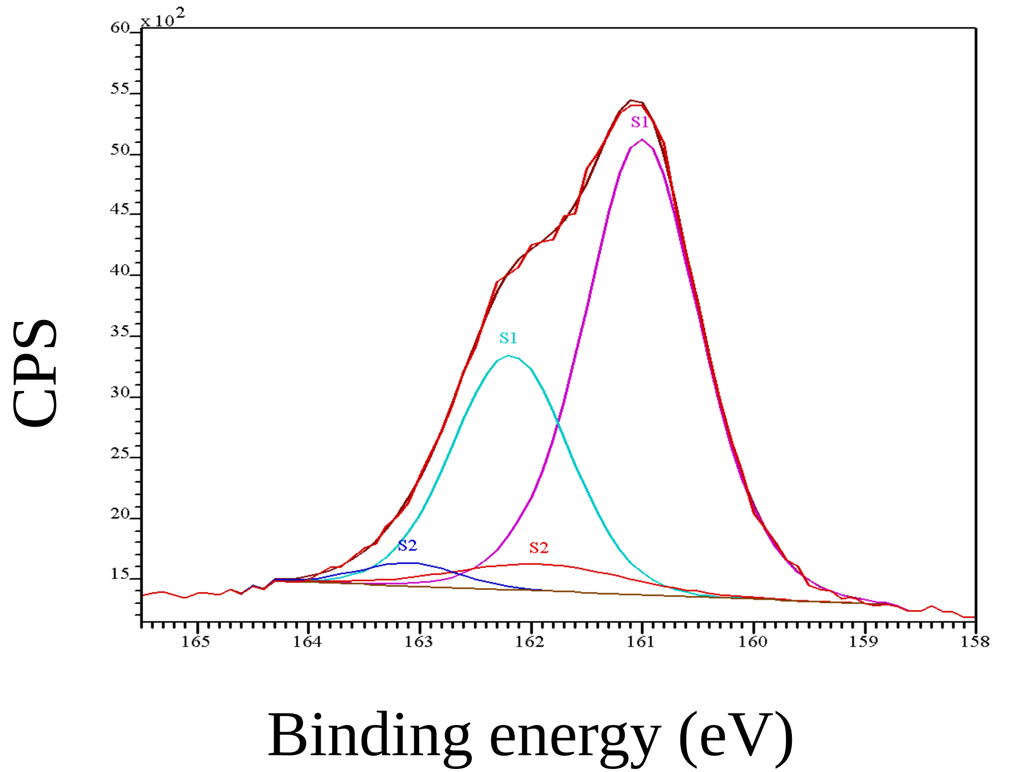

XPS S2p Core Peaks of the Li_6GeS_5 Target Material

E_b $S2p_{3/2-1/2}$	Experimental ratio	Theoretical ratio
161.1 – 162.3	NBS (~100 %)	NBS (80 %)
	0 %	Sulfide (20 %)

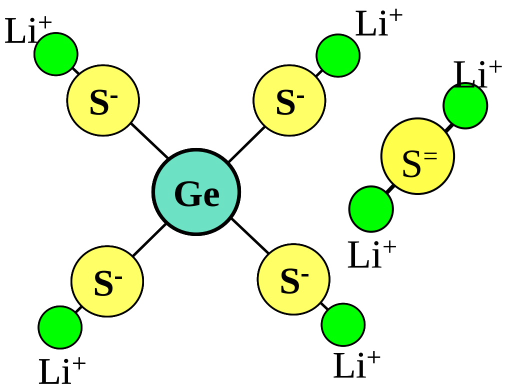

Li_4GeS_4 + Li_2S

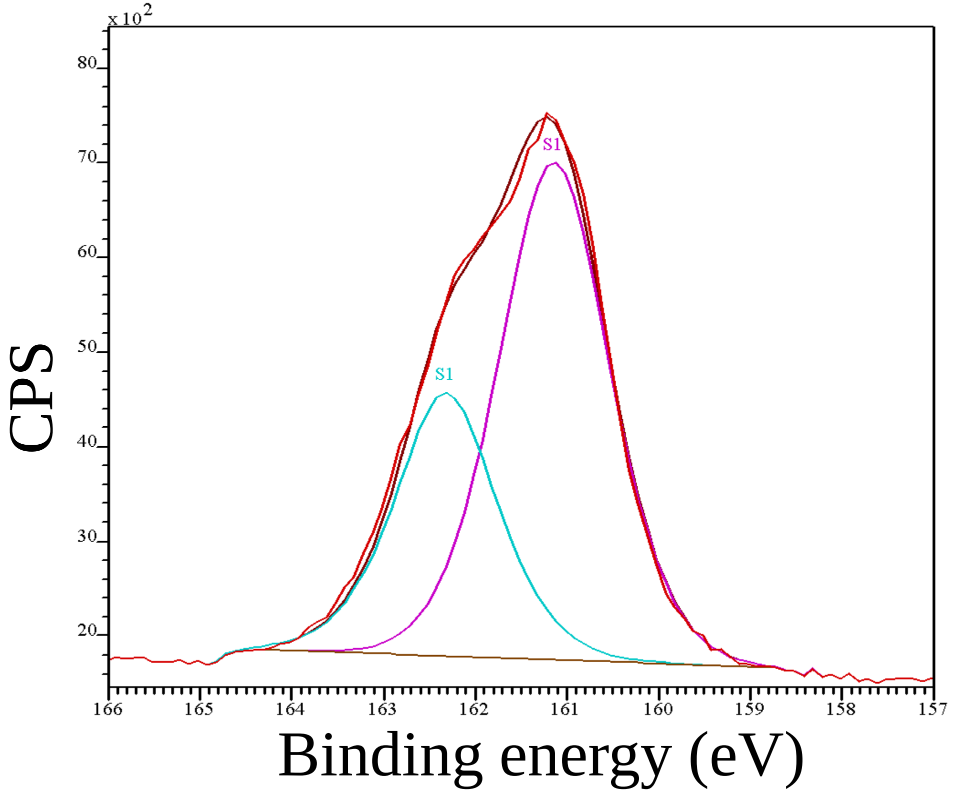

XPS S2p Core Peaks of the Starting Materials and Targets

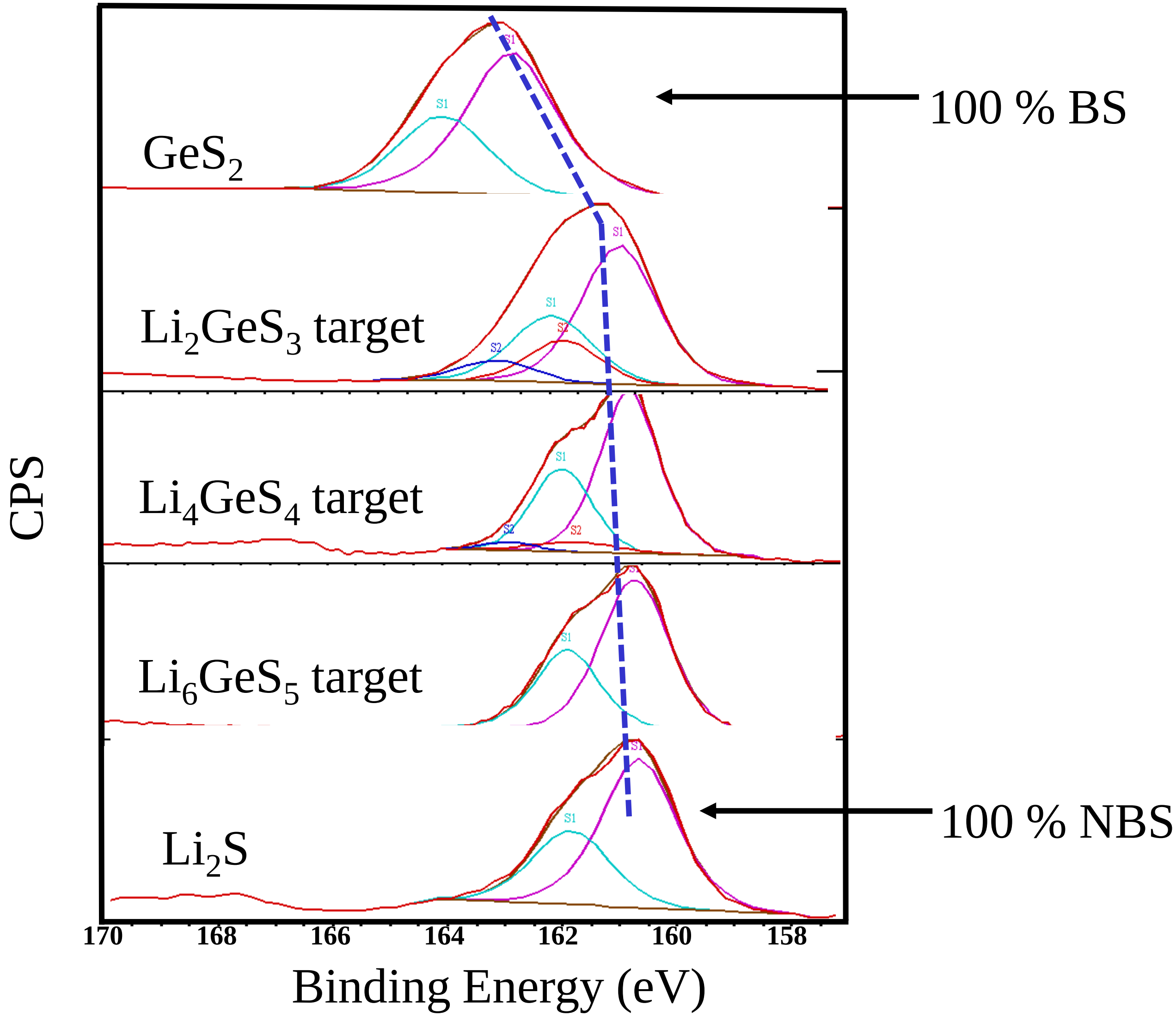

Compositions of the Li_2GeS_3 Thin film

(± 3 % error)

Li1s (0.028)	Ge2p3 (5.400)	S2p (0.717)	C1s (0.314)	O1s (0.733)	Comments (Sensitivity factor)
27.2	8.5	37.1	18.6	8.6	As prepared
32.6	15.9	47.8	0.0	3.7	Ar etching for 1 min.
31.7	16.1	48.1	0.0	4.1	Ar etching for 5 min.
33.3	16.7	50.0	0.0	0.0	Theoretical values

Merged XPS Spectra of the Li_2GeS_3 Thin Film

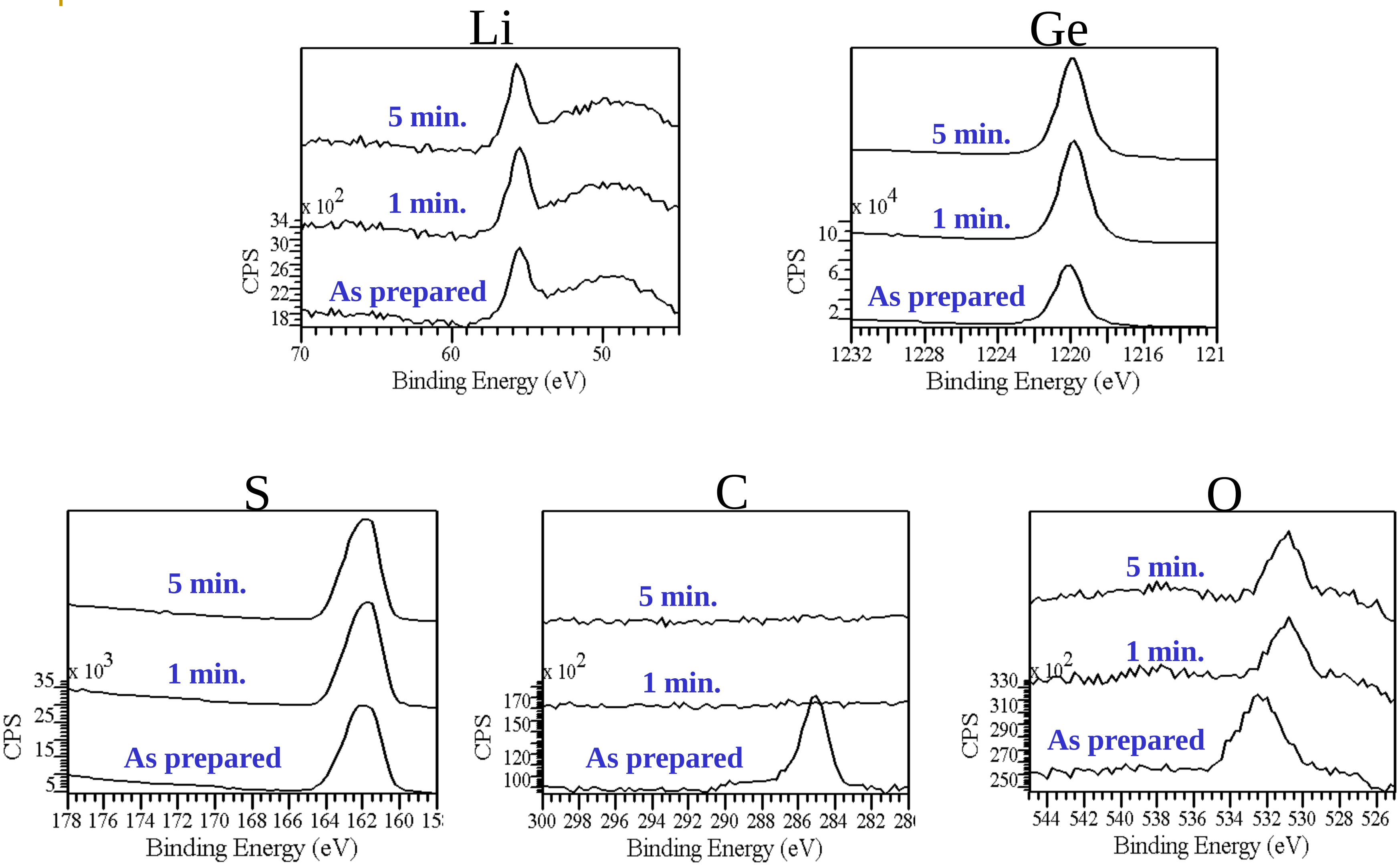

Compositions of the Li_4GeS_4 Thin Film

(± 3 % error)

Li1s (0.028)	Ge2p3 (5.400)	S2p (0.717)	C1s (0.314)	O1s (0.733)	Comments (Sensitivity factor)
31.0	5.5	32.1	18.3	13.1	As prepared
40.6	12.6	41.3	0.0	5.5	Ar etching for 1 min.
41.9	12.9	40.5	0.0	4.7	Ar etching for 5 min.
44.4	11.2	44.4	0.0	0.0	Theoretical values

Merged XPS Spectra of the Li_4GeS_4 Thin Film

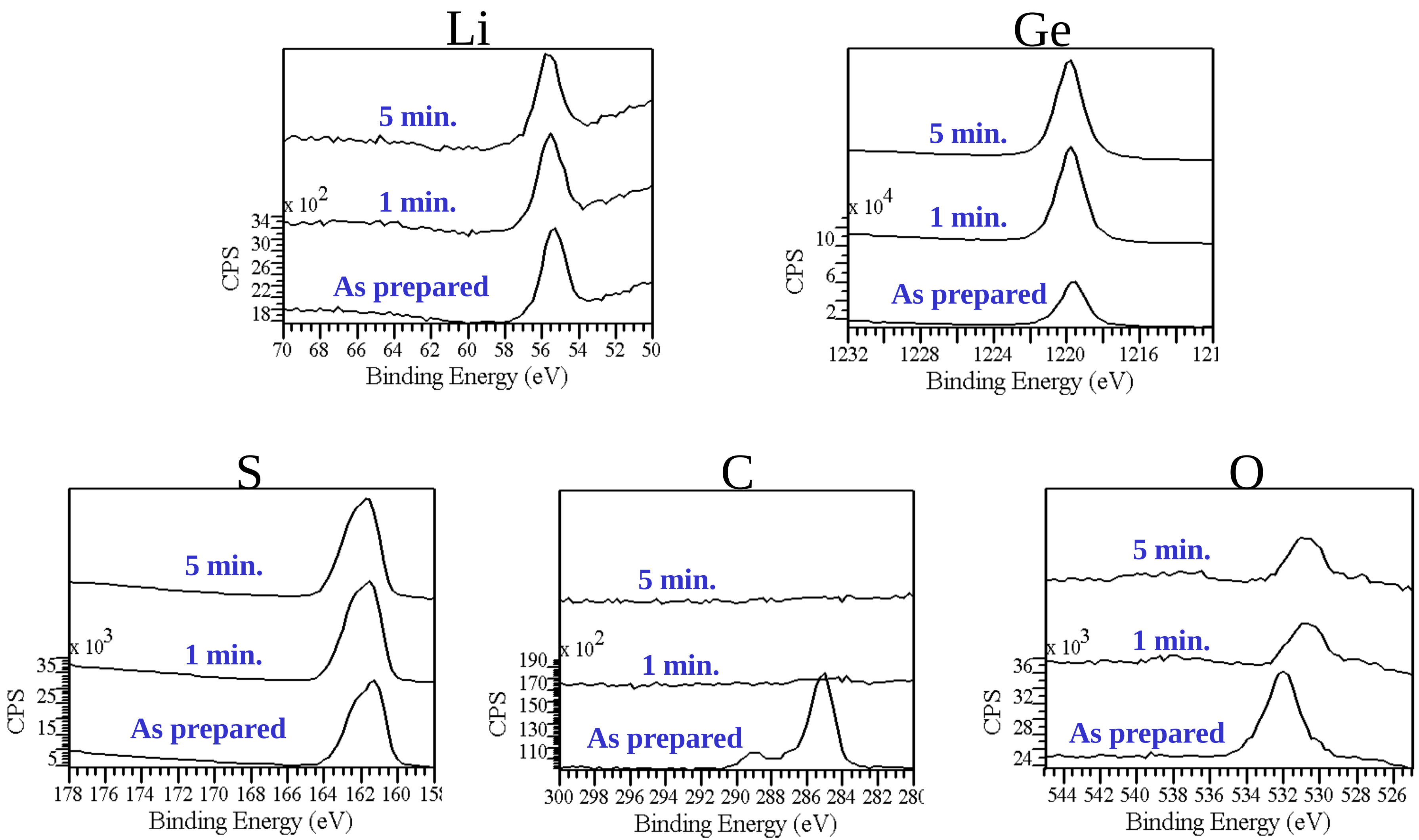

Compositions of the Li_6GeS_5 Thin Film

(± 3 % error)

Li1s (0.028)	Ge2p3 (5.400)	S2p (0.717)	C1s (0.314)	O1s (0.733)	Comments (Sensitivity factor)
35.9	4.9	33.2	14.7	11.3	As prepared
43.7	8.9	41.8	0.0	5.6	Ar etching for 1 min.
44.6	11.1	41.2	0.0	3.1	Ar etching for 5 min.
50.0	8.3	41.7	0.0	0.0	Theoretical values

Merged XPS Spectra of the Li_6GeS_5 Thin Film

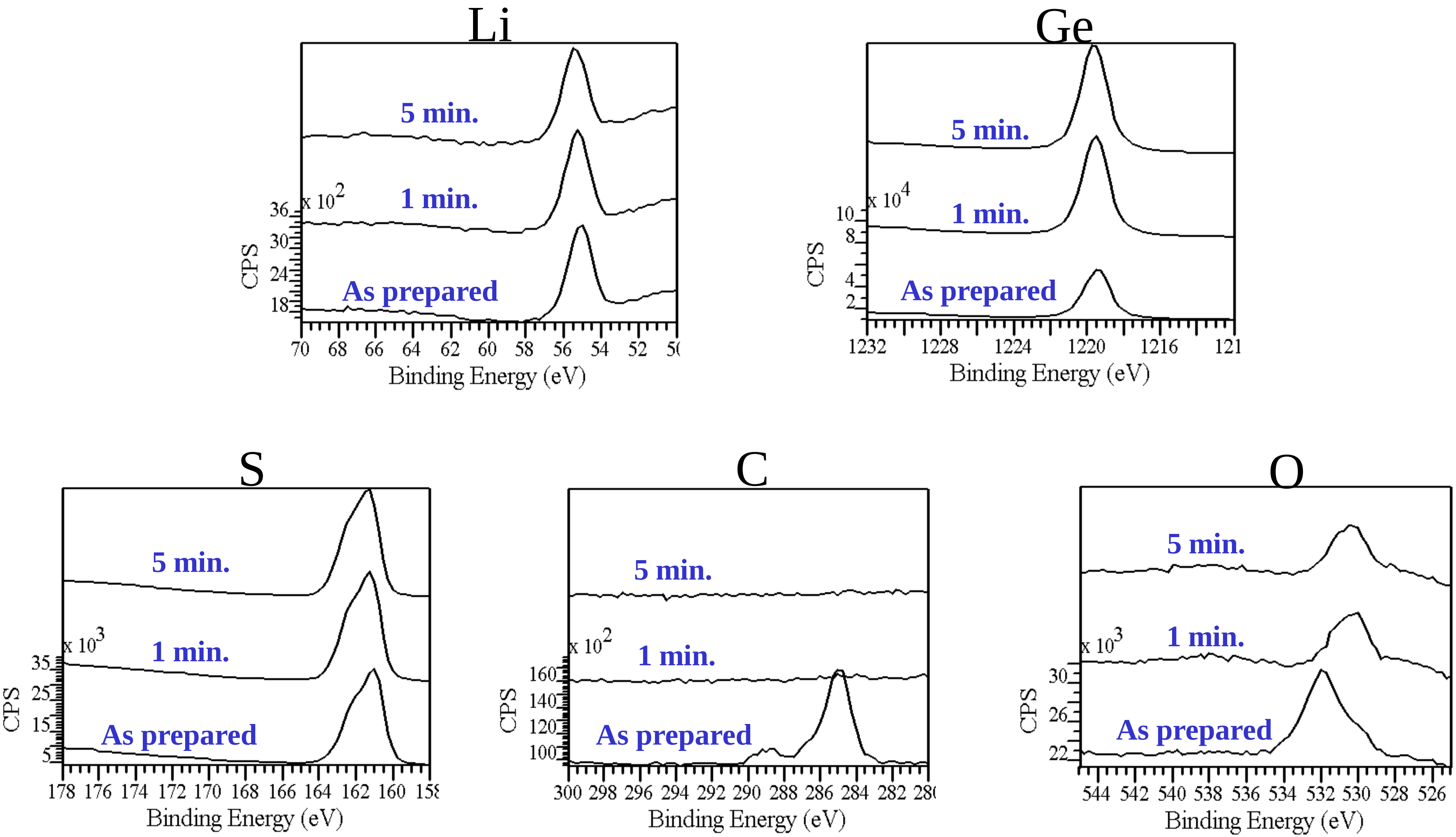

XPS S2p Core Peaks of the Starting Materials and Thin Films

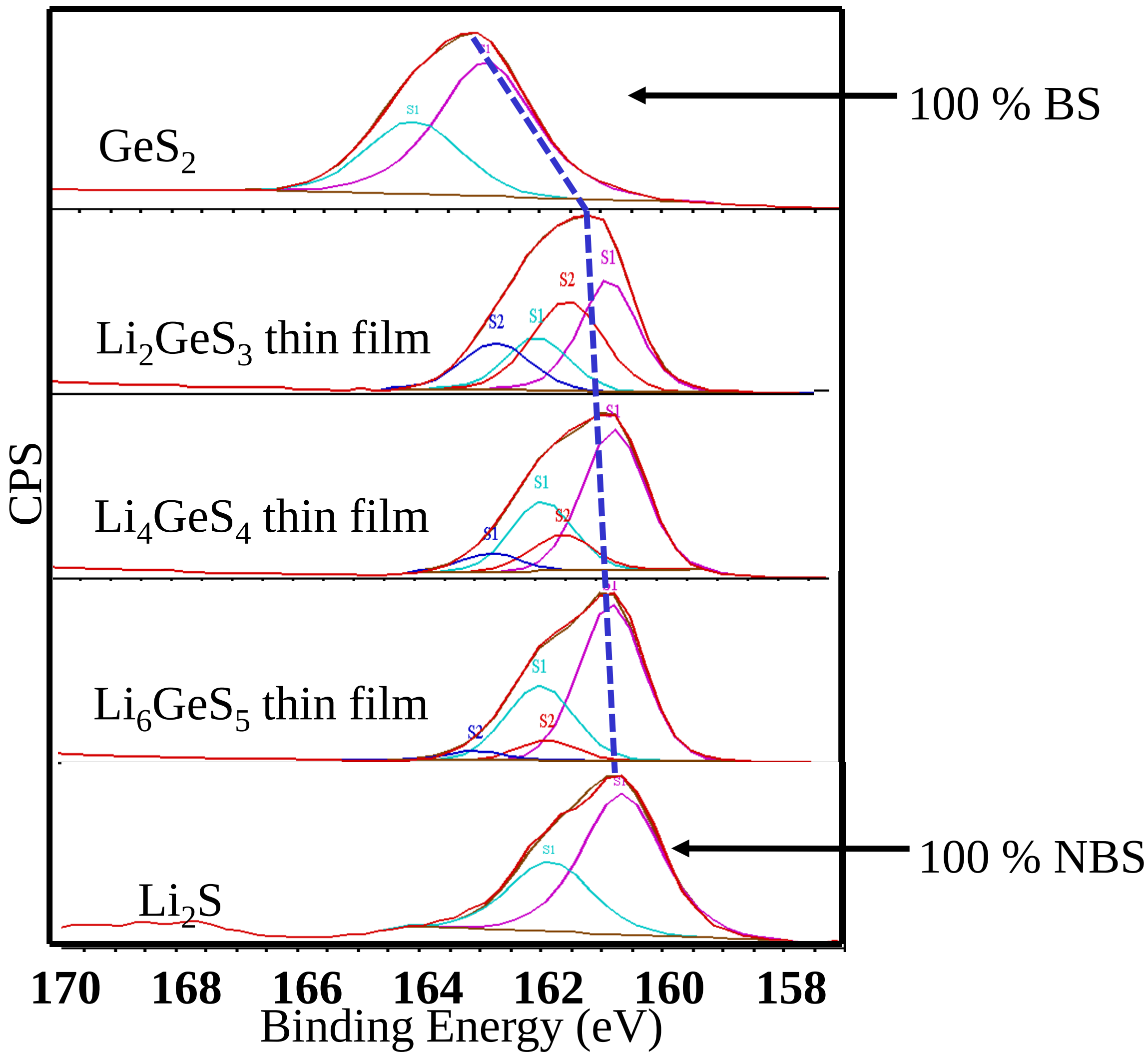

Sample Preparation of the Targets for Ionic Conductivity

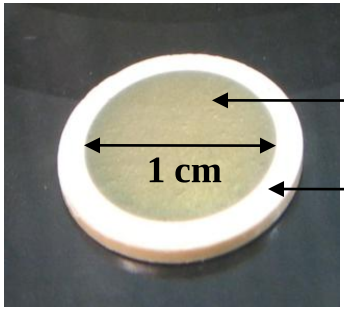

Sputtered Au electrode

Target (13 mm diameter)

Composition	Thickness (± 0.002 mm)	Area
Li_2GeS_3 target	0.96 mm	0.7854 cm^2
Li_4GeS_4 target	1.05 mm	0.7854 cm^2
Li_6GeS_5 target	0.85 mm	0.7854 cm^2

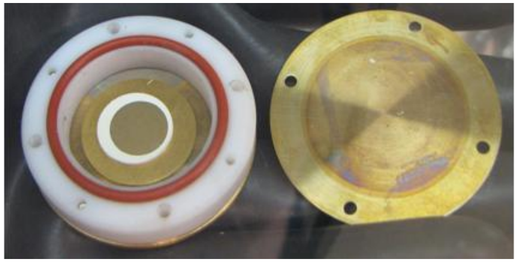

Before assembly

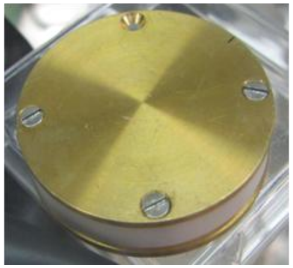

After assembly

Ionic Conductivities of the Li_2GeS_3 Target

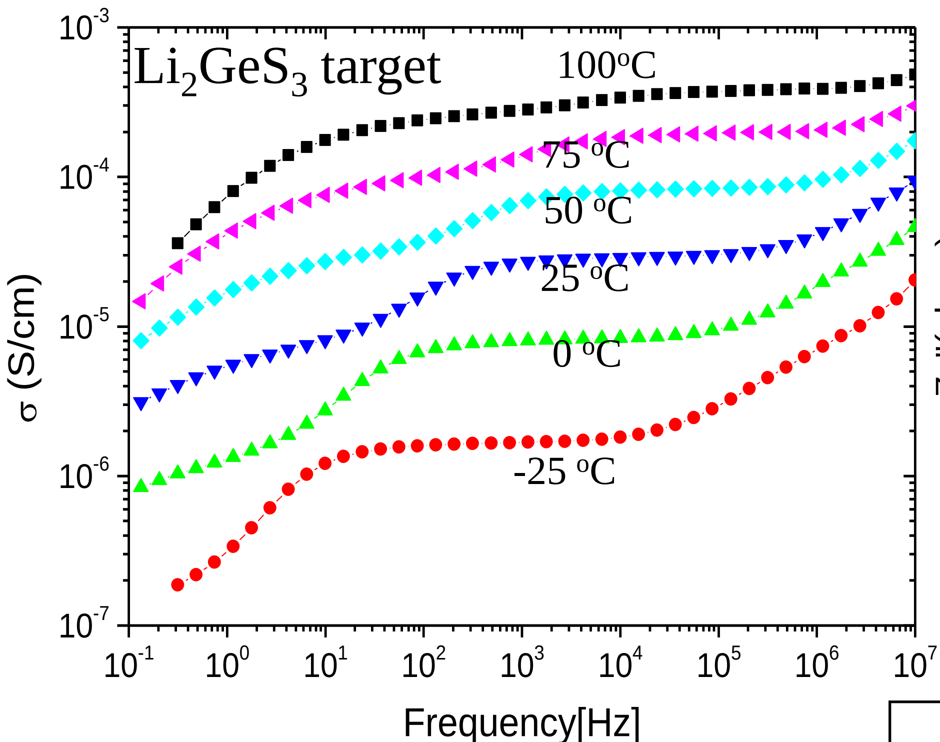

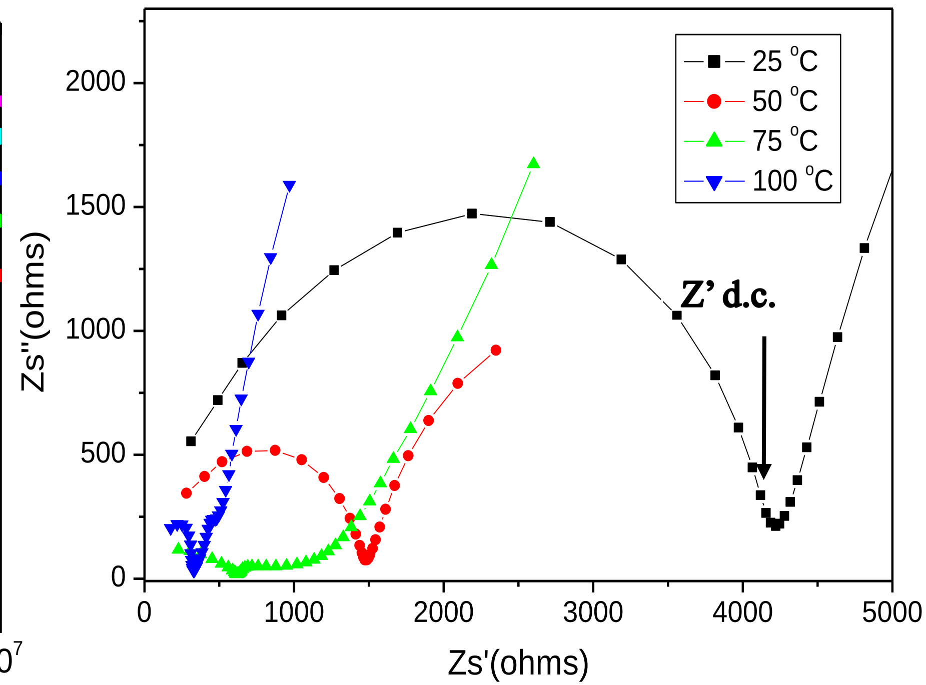

$$\sigma = \frac{1}{R} \times \frac{t}{A} = \frac{1}{R} \times \frac{0.096\ cm}{\sim 0.7854\ cm^2}$$

Temp. (°C)	Target resistance (Ω)	d.c. ionic conductivity (S/cm)
-25	7.3 (±100 Ω) × 10^{-4}	1.7 (±0.3) × 10^{-6}
0	1.5 (±70 Ω) × 10^{-4}	8.2 (±0.3) × 10^{-6}
25	4.2 (±50 Ω) × 10^{-3}	2.9 (±0.2) × 10^{-5}
50	1.5 (±40 Ω) × 10^{-3}	8.3 (±0.2) × 10^{-5}
75	6.2 (±20 Ω) × 10^{-2}	2.0 (±0.1) × 10^{-4}
100	3.2 (±10 Ω) × 10^{-2}	3.8 (±0.1) × 10^{-4}

Ionic Conductivities of the Li_4GeS_4 Target

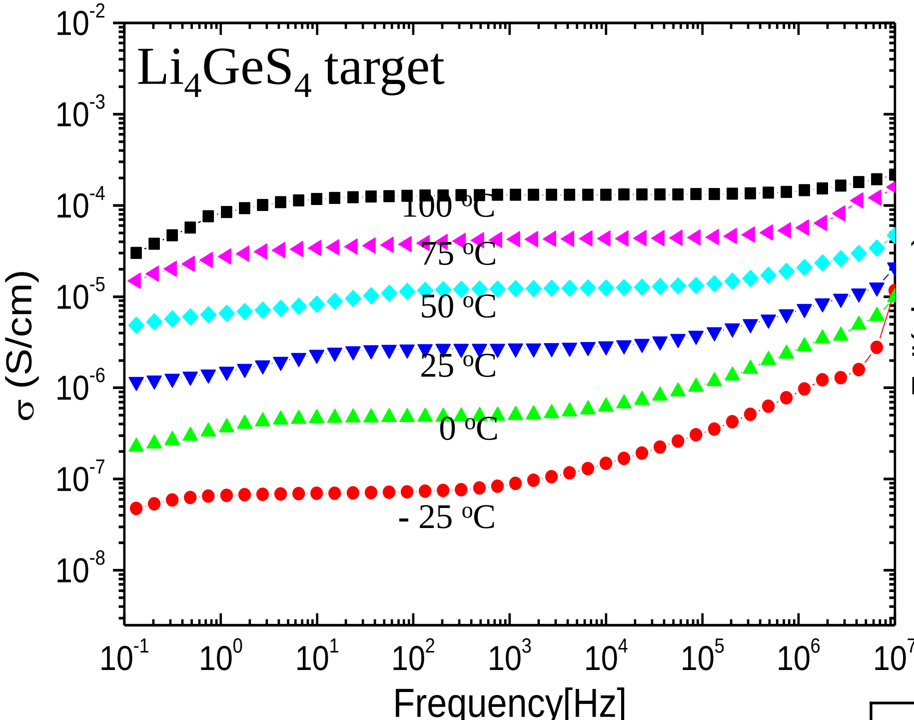

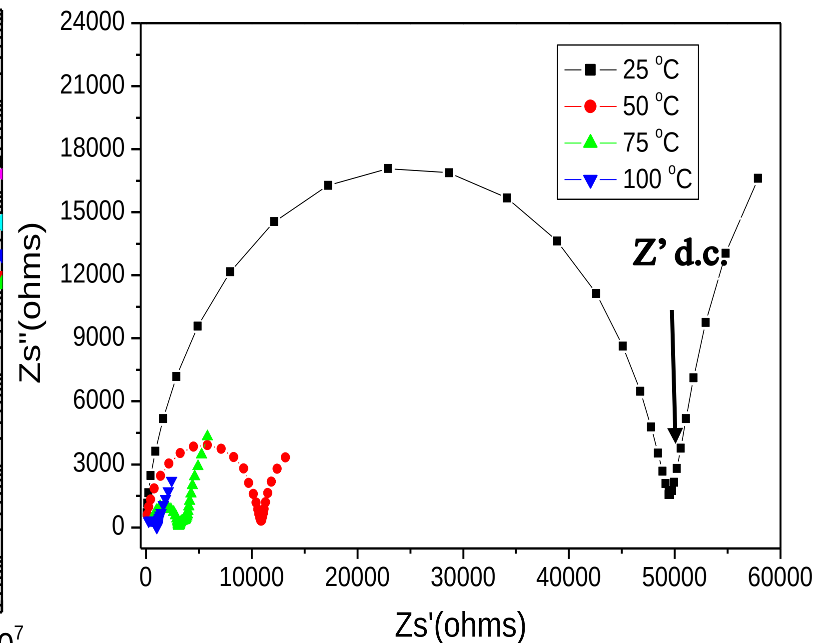

$$\sigma = \frac{1}{R} \times \frac{t}{A} = \frac{1}{R} \times \frac{0.105\ cm}{\sim 0.7854\ cm^2}$$

Temp. (°C)	Target resistance (Ω)	d.c. ionic conductivity (S/cm)
-25	1.9 (±500 Ω) × 10^6	7.0 (±0.5) × 10^{-8}
0	2.8 (±300 Ω) × 10^5	4.8 (±0.4) × 10^{-7}
25	4.9 (±100 Ω) × 10^4	2.7 (±0.3) × 10^{-6}
50	1.1 (±80 Ω) × 10^4	1.2 (±0.2) × 10^{-5}
75	3.1 (±50 Ω) × 10^3	4.3 (±0.2) × 10^{-5}
100	1.0 (±30 Ω) × 10^3	1.3 (±0.1) × 10^{-4}

Ionic Conductivities of the Li_6GeS_5 Target

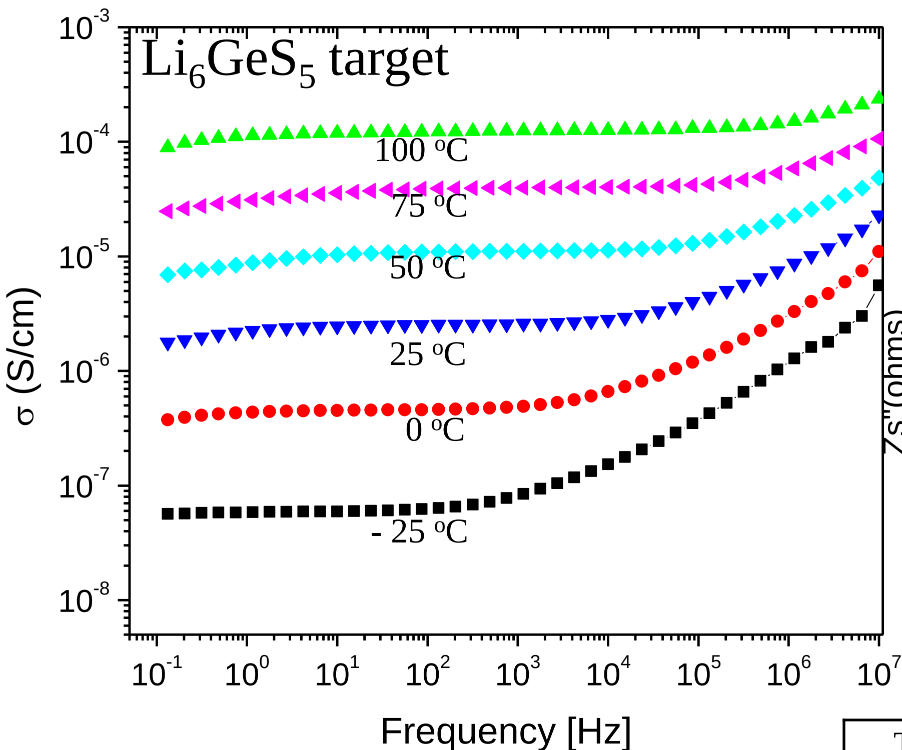

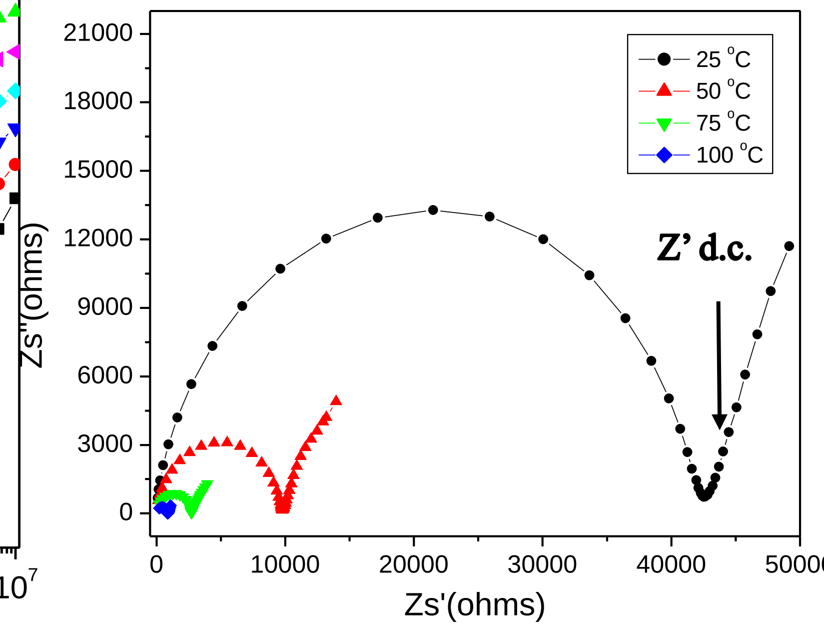

$$\sigma = \frac{1}{R} \times \frac{t}{A} = \frac{1}{R} \times \frac{0.085\ cm}{\sim 0.7854\ cm^2}$$

Temp. (ºC)	Target resistance (Ω)	d.c. ionic conductivity (S/cm)
-25	1.8 (±500 Ω) × 10^6	5.9 (±0.5) × 10^{-8}
0	2.4 (±300 Ω) × 10^5	4.5 (±0.4) × 10^{-7}
25	4.2 (±100 Ω) × 10^4	2.5 (±0.3) × 10^{-6}
50	9.8 (±80 Ω) × 10^3	1.1 (±0.2) × 10^{-5}
75	2.7 (±50 Ω) × 10^3	4.0 (±0.2) × 10^{-5}
100	8.6 (±25 Ω) × 10^2	1.3 (±0.1) × 10^{-4}

Arrhenius Plots of the d.c. Conductivity of the Targets

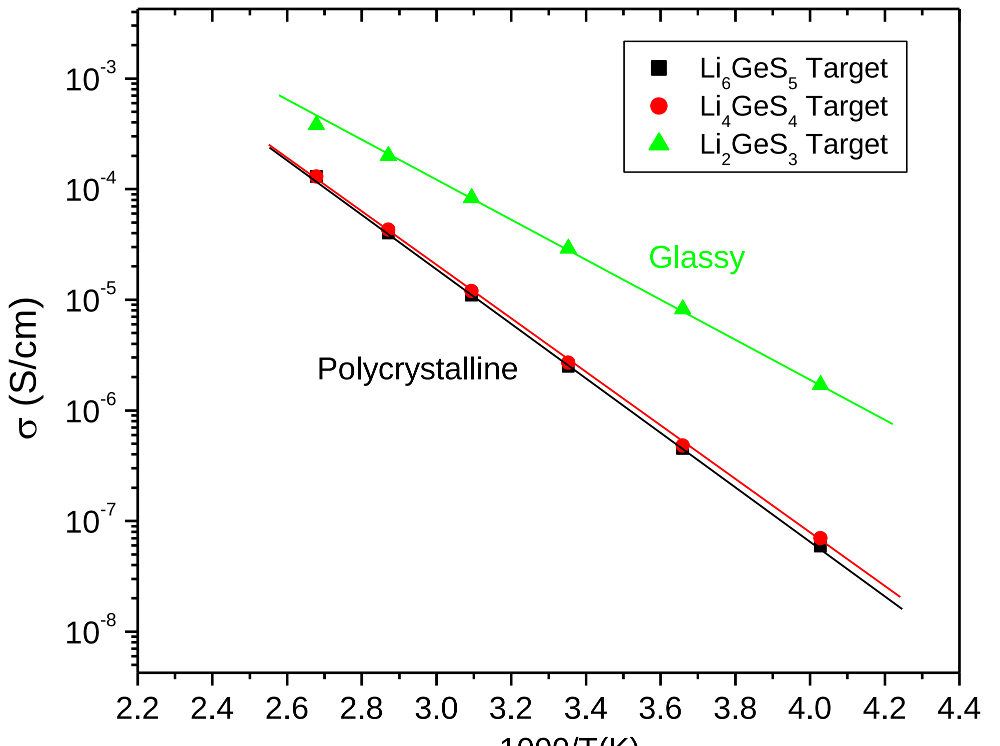

Composition	$\sigma_{25°C}$ (S/cm)	ΔE_a (eV) (± 0.005)	Logσ_o (S/cm) (± 0.005)
Li_2GeS_3 target	2.9×10^{-5}	0.337	1.135
Li_4GeS_4 target	2.7×10^{-6}	0.492	2.764
Li_6GeS_5 target	2.5×10^{-6}	0.497	2.828

Sample Preparation of the Thin Film for Ionic Conductivity

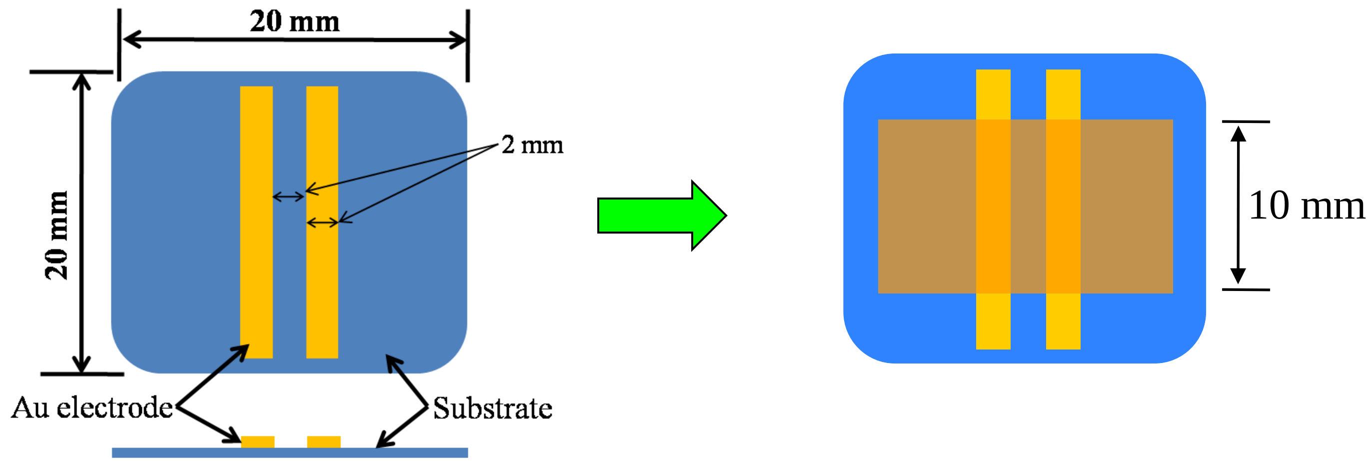

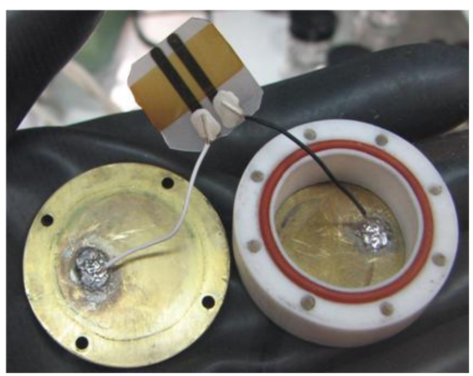

Before assembly

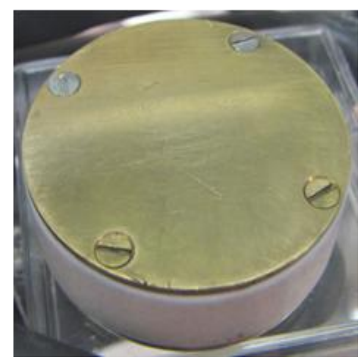

After assembly

Ionic Conductivities of the Li_2GeS_3 Thin Film

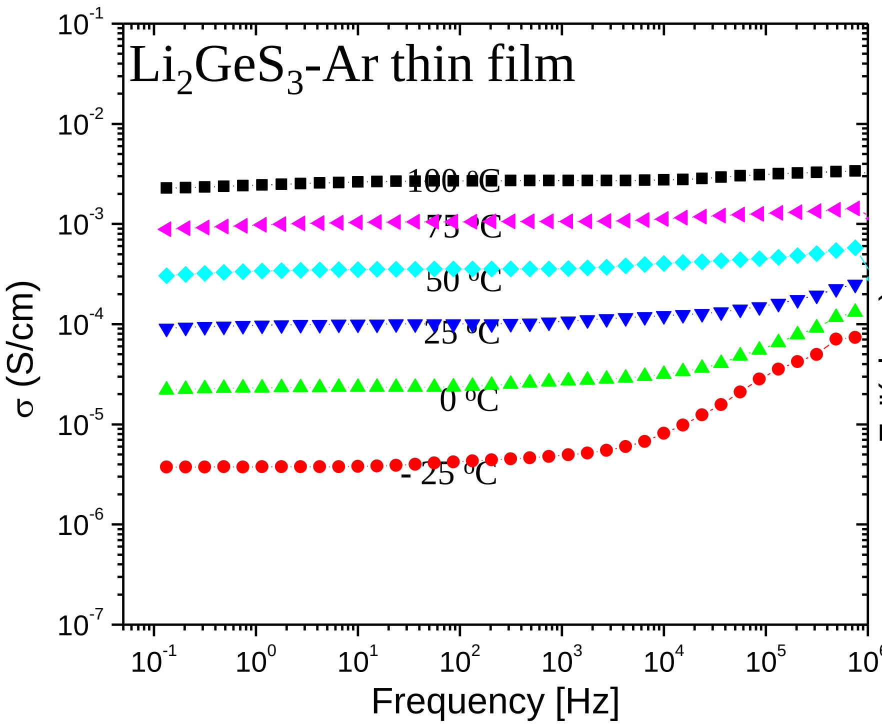

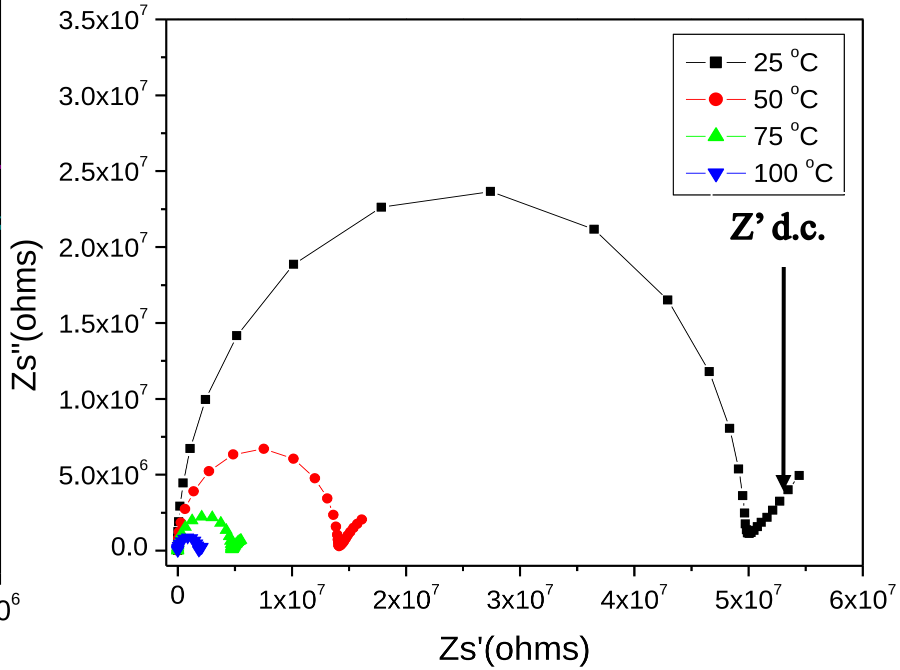

$$\sigma = \frac{1}{R} \times \frac{t}{A} = \frac{1}{R} \times \frac{0.2\,cm}{\sim 0.00004\ cm^2}$$

Temp. (°C)	Thin film resistance (Ω)	d.c. ionic conductivity (S/cm)
-25	1.3×10^9	$4.0\ (\pm 0.3) \times 10^{-6}$
0	2.1×10^8	$2.5\ (\pm 0.2) \times 10^{-5}$
25	5.0×10^7	$1.1\ (\pm 0.1) \times 10^{-4}$
50	1.4×10^7	$3.8\ (\pm 0.1) \times 10^{-4}$
75	4.8×10^6	$1.1\ (\pm 0.05) \times 10^{-3}$
100	1.8×10^6	$2.9\ (\pm 0.05) \times 10^{-3}$

Ionic Conductivities of the Li_4GeS_4 Thin Film

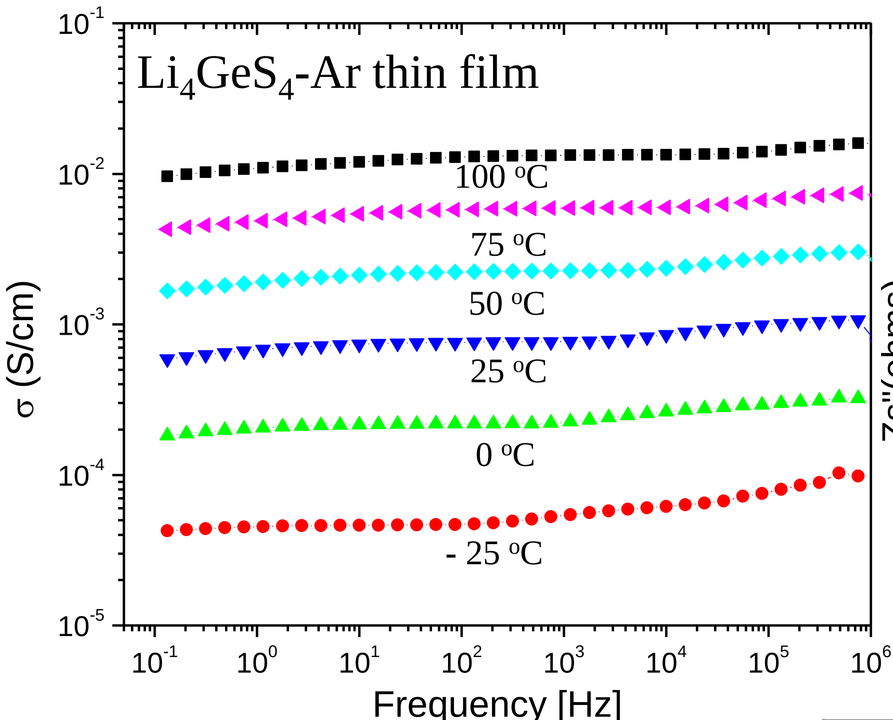

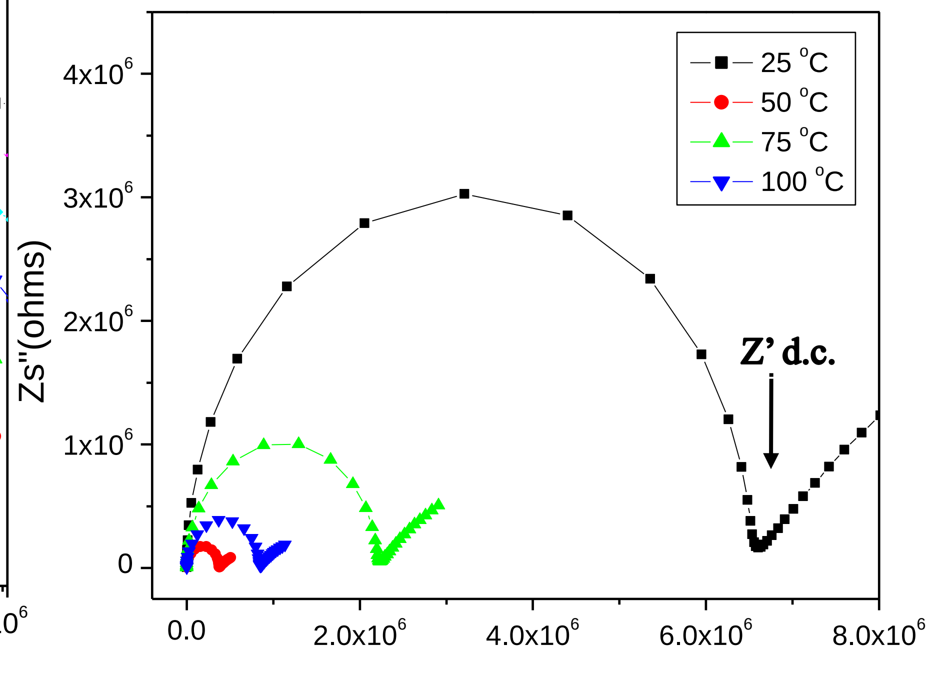

$$\sigma = \frac{1}{R} \times \frac{t}{A} = \frac{1}{R} \times \frac{0.2\,cm}{\sim 0.00004\ cm^2}$$

Temp. (°C)	Target resistance (Ω)	d.c. ionic conductivity (S/cm)
-25	1.0×10^8	$4.6 (\pm 0.2) \times 10^{-5}$
0	2.3×10^7	$2.2 (\pm 0.1) \times 10^{-4}$
25	6.6×10^6	$7.5 (\pm 0.1) \times 10^{-4}$
50	2.2×10^6	$2.2 (\pm 0.05) \times 10^{-3}$
75	8.5×10^5	$5.8 (\pm 0.05) \times 10^{-3}$
100	3.8×10^5	$1.3 (\pm 0.02) \times 10^{-2}$

Ionic Conductivities of the Li_6GeS_5 Thin Film

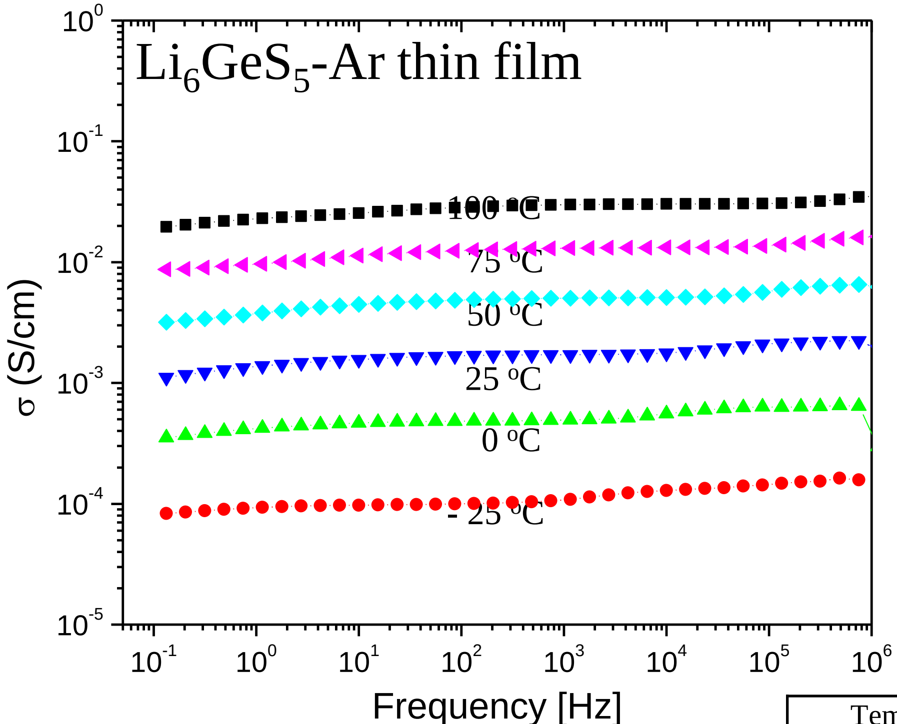

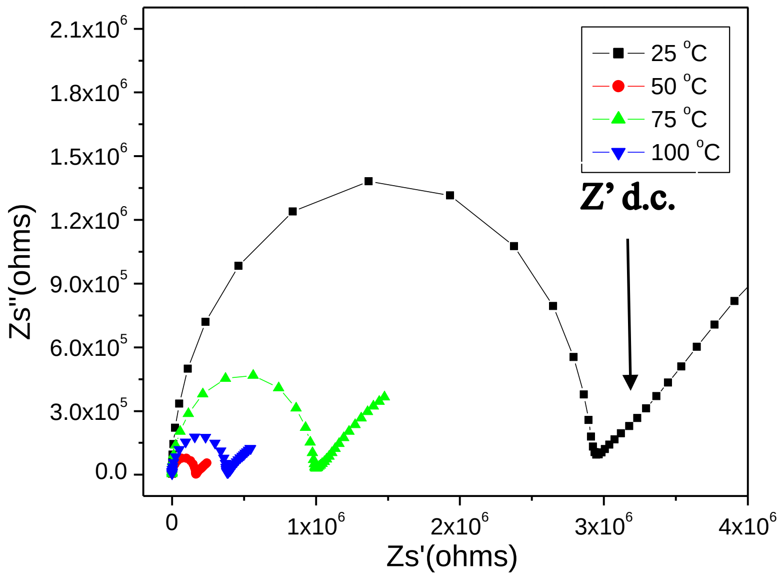

$$\sigma = \frac{1}{R} \times \frac{t}{A} = \frac{1}{R} \times \frac{0.2\,cm}{\sim 0.00004\ cm^2}$$

Temp. (ºC)	Target resistance (Ω)	d.c. ionic conductivity (S/cm)
-25	5.1×10^7	$9.7 (\pm 0.2) \times 10^{-5}$
0	1.0×10^7	$4.8 (\pm 0.1) \times 10^{-4}$
25	2.9×10^6	$1.7 (\pm 0.05) \times 10^{-3}$
50	1.0×10^6	$5.0 (\pm 0.05) \times 10^{-3}$
75	3.8×10^5	$1.3 (\pm 0.02) \times 10^{-2}$
100	1.6×10^5	$3.0 (\pm 0.02) \times 10^{-2}$

Arrhenius Plots of d.c. Ionic Conductivity of the Thin Films

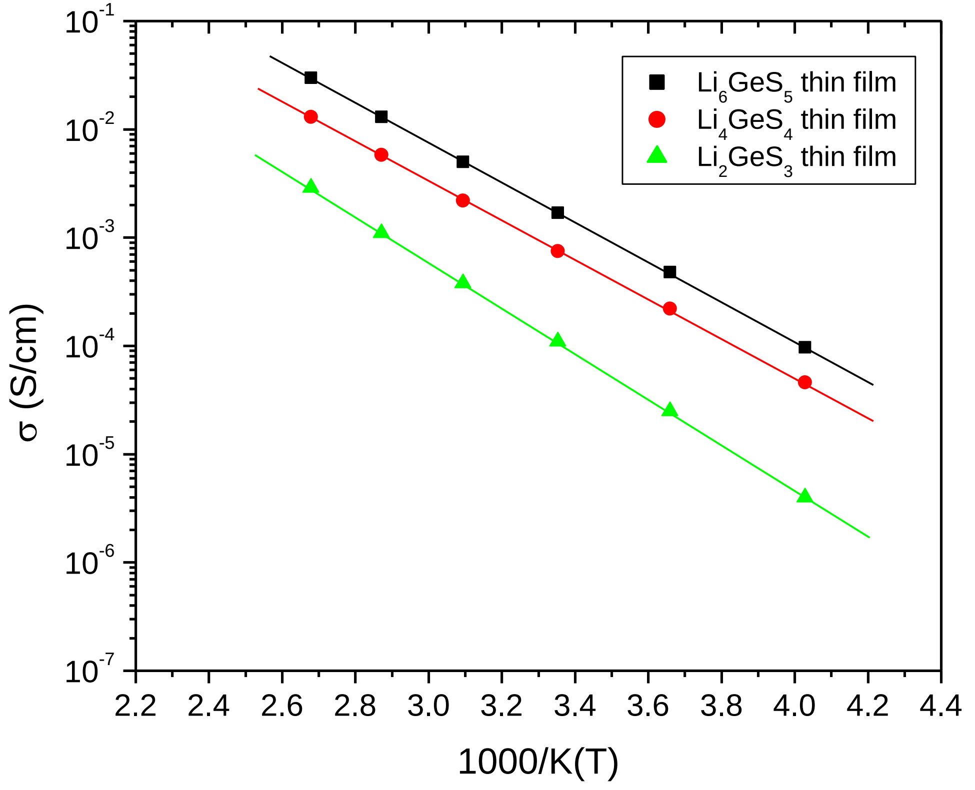

Composition	$\sigma_{25°C}$ (S/cm)	ΔE_a (eV) (± 0.005)	$\text{Log}\sigma_o$ (S/cm) (± 0.005)
Li_2GeS_3-Ar thin film	1.1 (±0.1) × 10^{-4}	0.417	3.096
Li_4GeS_4-Ar thin film	7.5 (±0.1) × 10^{-4}	0.358	2.951
Li_6GeS_5-Ar thin film	1.7 (±0.05) × 10^{-3}	0.363	3.382

Arrhenius Plots of the Ionic Conductivities of the Thin Films

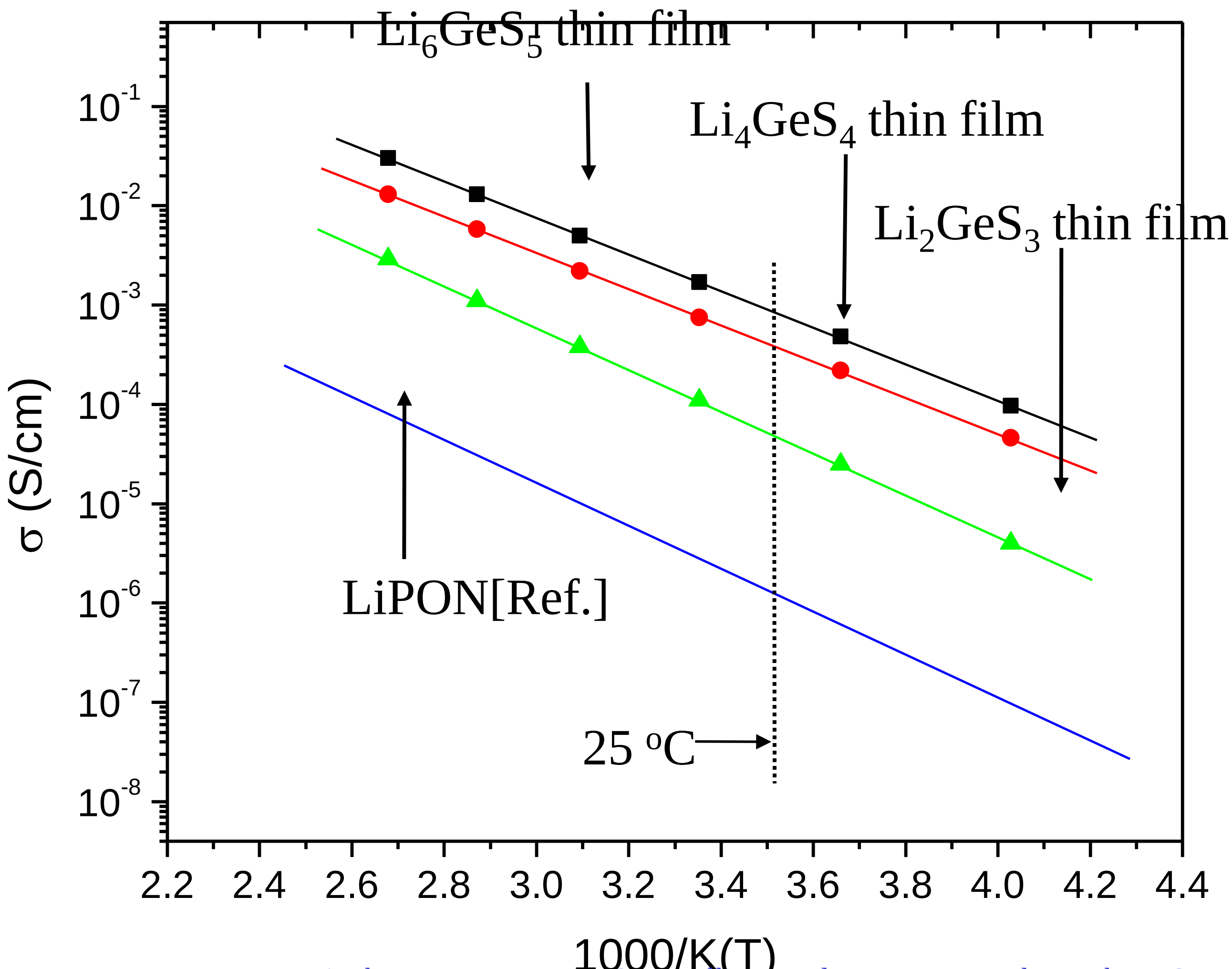

Xiaohua Yu, J. B. Bates, G. E. Jellison and F. X. Hart, J. Electrochem. Soc. Vol 144, 2 (1997) 524.

Arrhenius Plots of the Ionic Conductivities of Targets and Thin Films

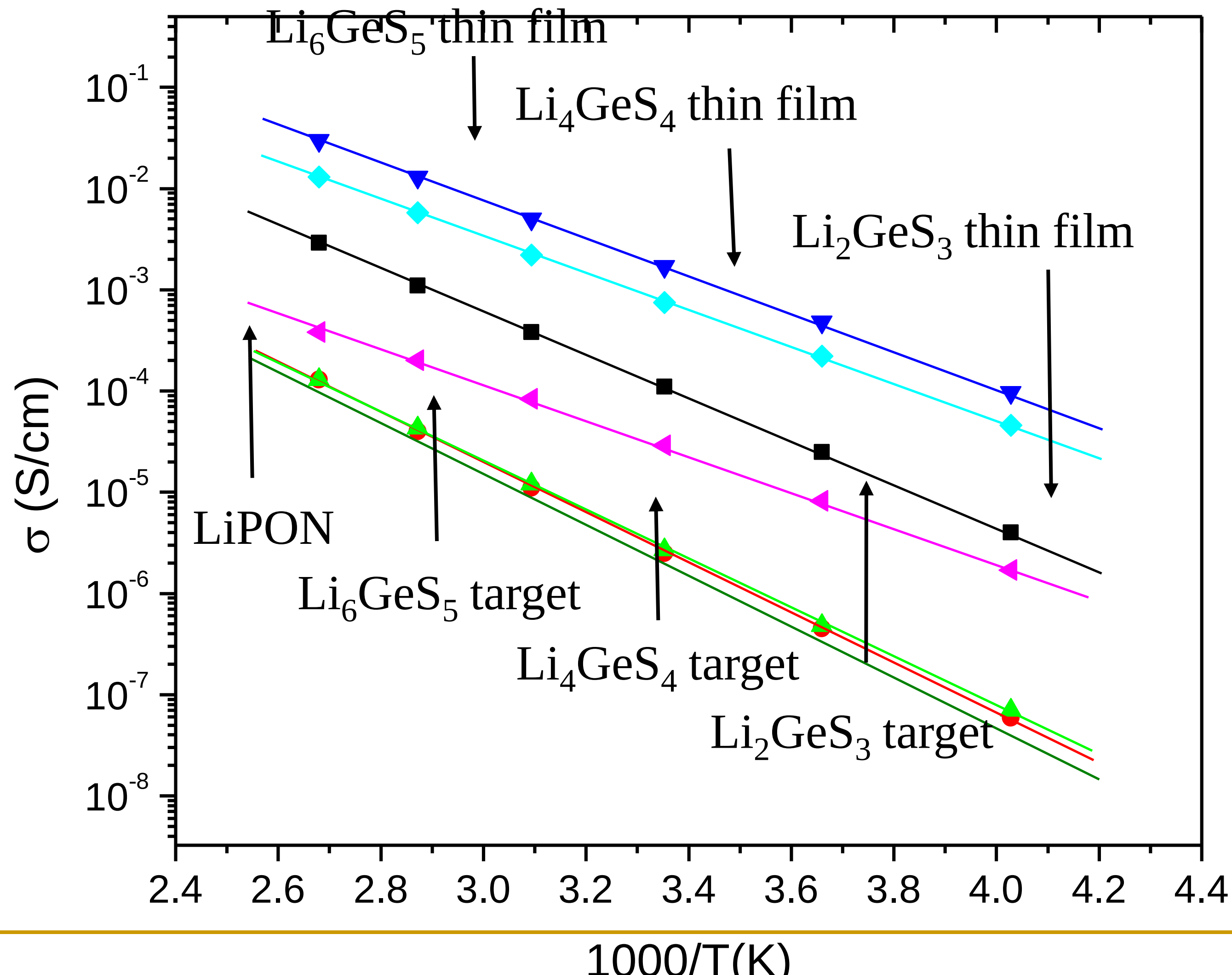

Ionic Conductivities of Li_4GeS_4 Thin Films under various Conditions

Li_4GeS_4 thin film	Sputtering time	Pressure	Power	Width	Space	Thickness (microns)	k = t/A (cm^{-1})
(a)	90	30	45W	10 mm	2 mm	0.5	4,000
(b)	90	25	45W	10 mm	2 mm	0.5	4,000
(c)	30	25	50W	10 mm	3 mm	0.17	17,647
(d)	30	25	50W	10 mm	2 mm	0.17	11,765

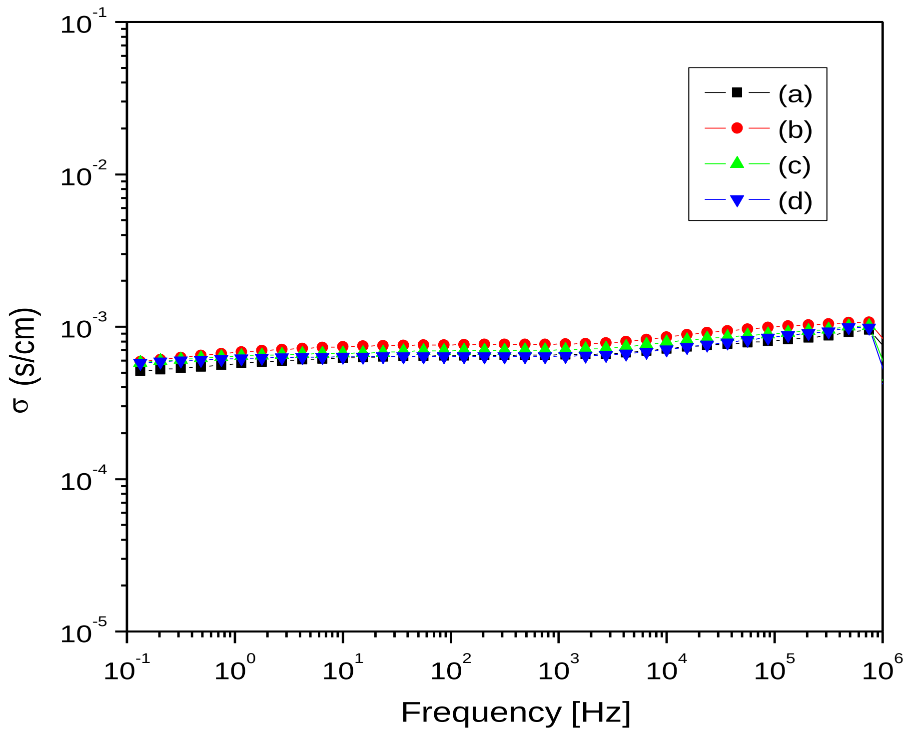

Summary and Conclusions

- We have successfully made nLi_2S+GeS_2(n=1, 2 and 3) thin films in Ar atmosphere.
- From the SEM data, the thin films showed high quality surface morphology.
- Raman and IR data showed consistent structures between targets and thin films.
- Target XPS compositional data are close to thin film composition and both closely match theoretical values. In addition, C exists only 1 nm from the surface and minor O exists 1 nm below the surface.
- The ionic conductivities of thin films at RT are 100 to 1000 times larger than oxide thin films (LiPON) which are the current commercial products.
  In addition, the thin films are thermally stable up to 100 ^oC
- The lithium thio-germanate thin film electrolytes are very promising for solid state Li-ion batteries.

Acknowledgements –
ISU Glass and Optical Materials Research Group

Future work (Ge based system)

- Add GeO_2 to $nLi_2S + GeS_2$ system to increase chemical stability (and Li+ ion conductivity?)
- Use an $Ar + N_2$ atmosphere for sputtering to increase ionic conductivity of the thin film electrolytes (and stabilize electrolyte-lithium interface?)
- Test lithium thin-film solid state batteries with lithium anodes and transition metal oxide cathodes

Concluding comment…..

It's all we've got…..let's take good care of it….